

2019

Development of potential strategies for DNA quantification and DNA probes for detection of Legionella pneumophila

Parker James Dulin
Iowa State University

Follow this and additional works at: <https://lib.dr.iastate.edu/etd>



Part of the [Civil Engineering Commons](#), and the [Environmental Engineering Commons](#)

Recommended Citation

Dulin, Parker James, "Development of potential strategies for DNA quantification and DNA probes for detection of Legionella pneumophila" (2019). *Graduate Theses and Dissertations*. 17673.
<https://lib.dr.iastate.edu/etd/17673>

This Thesis is brought to you for free and open access by the Iowa State University Capstones, Theses and Dissertations at Iowa State University Digital Repository. It has been accepted for inclusion in Graduate Theses and Dissertations by an authorized administrator of Iowa State University Digital Repository. For more information, please contact digirep@iastate.edu.

**Development of potential strategies for DNA quantification and DNA probes for detection
of *Legionella pneumophila***

by

Parker James Dulin

A thesis submitted to the graduate faculty
in partial fulfillment of the requirements for the degree of
MASTER OF SCIENCE

Major: Civil Engineering (Environmental Engineering)

Program of Study Committee:
Kaoru Ikuma, Co-major Professor
Carmen Gomes, Co-major Professor
Chris Rehmann

The student author, whose presentation of the scholarship herein was approved by the program of study committee, is solely responsible for the content of this thesis. The Graduate College will ensure this thesis is globally accessible and will not permit alterations after a degree is conferred.

Iowa State University

Ames, Iowa

2019

Copyright © Parker James Dulin, 2019. All rights reserved.

TABLE OF CONTENTS

	Page
LIST OF FIGURES	iv
LIST OF TABLES	vi
NOMENCLATURE	vii
ACKNOWLEDGMENTS	viii
ABSTRACT.....	ix
CHAPTER 1. GENERAL INTRODUCTION	1
Methods of Detection for Waterborne Pathogens	2
Opportunistic Premise Plumbing Pathogens	4
Biosensors.....	7
DNA Quantification	13
DNA Hybridization	16
Scope of Research	18
References	19
CHAPTER 2. METHODS FOR ACCURATE QUANTIFICATION OF STRUCTURED DNA PROBES AND DOUBLE-STRANDED DNA AFTER HYBRIDIZATION USING THE QUBIT FLUOROMETER.....	27
Abstract.....	27
Introduction	28
Procedures	31
Quantification of Structured DNA Probes	32
Quantification of DNA Hybridization.....	35
Additional Information and Method Validation.....	36
Conclusions	42
References	43
CHAPTER 3. THE EFFECT OF STRUCTURE ON DNA HYBRIDIZATION IN SOLUTION AND IMMOBILIZED ON A PARTICLE SURFACE FOR OPTIMIZED DETECTION OF <i>LEGIONELLA PNEUMOPHILA</i>	46
Abstract.....	46
Introduction	47
Materials and Methods	49
Solution Study	52
Particle Study	55
Statistical Analysis	60
Results and Discussion	60
Solution Study	60
Characterization of DNA Conjugated Magnetic Particles and Immobilized Hybridization Conditions	65

Particle Study	66
Conclusions	68
References	69
CHAPTER 4. GENERAL CONCLUSIONS.....	73
Engineering Significance.....	74
Future Recommendations	75
APPENDIX. PCR PROTOCOLS.....	77
References	79

LIST OF FIGURES

	Page
Figure 1.1. Reported cases of Legionnaires' disease since the beginning of the 21 st century.....	5
Figure 1.2. Diagram of the two major components of a biosensor.....	8
Figure 1.3. Example of a sandwich DNA hybridization strategy for biosensing detection.....	9
Figure 1.4. Schematic of a potential microfluidic device for an electrochemical DNA-based biosensor.....	12
Figure 1.5. Examples of DNA motifs that are available through intramolecular and intermolecular interactions.	17
Figure 2.1. Schematic of the process for quantification of structured DNA probes via denaturation with DMSO followed by fluorescent dye treatment.....	31
Figure 2.2. Schematic of the process for quantification of DNA hybridization via enzymatic digestion followed by fluorescent dye treatment.....	34
Figure 2.3. Comparison between ssDNA concentrations measured with Qubit and NanoDrop.	37
Figure 2.4. Linear calibration for the determination of ssDNA concentration dissolved in DMSO.....	39
Figure 2.5. Measured concentrations of dsDNA spiked with concentrations of ssDNA to assess the effect of ssDNA on background noise.	40
Figure 2.6. Concentrations of dsDNA spiked with concentrations of ssDNA and treated with Exonuclease I.	42
Figure 3.1. Linear calibration for the determination of ssDNA concentration dissolved in DMSO.....	53
Figure 3.2. Linear calibration curve for quantification of dsDNA in the presence of ssDNA, enzymes used for cleanup, and respective buffers.	54
Figure 3.3. Linear calibration of each DNA probe for their quantification after particle immobilization.....	56
Figure 3.4. Linear calibration for quantification of magnetic particles based on measurement of optical density (OD).....	57

Figure 3.5. Raw RFU measurements from LSP, Key, and the respective scrambled sequences when exposed to incrementally increased copies of TS.....	61
Figure 3.6. Sequences of hybridized duplexes for LSP (top) and Key (bottom) with the probe sequences in black and the TS in red.	62
Figure 3.7. Percent hybridization achieved by LSP and Key when exposed to incremental copies of TS.....	63
Figure 3.8. Hybridization efficiency for DNA immobilized (Bio-Key and Bio-LSP) on particles at increasing availability of TS.	67
Figure 4.1. Schematic of microfluidic device enabled for magnetic separation followed by electrochemical biosensing.....	75

LIST OF TABLES

	Page
Table 1.1. OPPPs screened at various locations in the school via PCR and electrophoresis gels.....	6
Table 3.1. List of the DNA sequences employed for all aspects of this study.	51
Table 3.2. Linear regressions for the raw RFU measurements associated with each probe at increasing concentration of TS.....	61
Table 3.3. Characteristics of functionalized magnetic particles (MP) after DNA immobilization.....	66
Table A.1. Protocols	77

NOMENCLATURE

OPPP	Opportunistic Premise Plumbing Pathogen
PCR	Polymerase Chain Reaction
ssDNA	Single-stranded DNA
dsDNA	Double-stranded DNA
RFUs	Relative Fluorescence Units
NaOH	Sodium Hydroxide
DMSO	Dimethyl Sulfoxide
TS	Target Strand
LSP	Linear Signal Probe
Key	Dangling-ended Hairpin Probe

ACKNOWLEDGMENTS

I would like to thank my major professors, Dr. Kaoru Ikuma and Dr. Carmen Gomes, and my committee member, Dr. Chris Rehmann, for their guidance, support, and insight throughout the course of this research. I am thankful for the opportunity to participate in this research and work in a laboratory filled with passionate, thoughtful, and intelligent students. I would like to thank the students of the Ikuma Lab Group, Sahar Daer, Meesha Legg, Xuewei Liang, and Rayla Vilar, for their support and assistance with this research.

In addition, I would also like to thank my friends, colleagues, the department faculty and staff for making my time at Iowa State University an unforgettable experience. I want to also offer my appreciation to the school system willing to participate in my study, without whom, this thesis would not have been possible.

ABSTRACT

After the Flint Water Crisis, there has been heightened public awareness on threats to potable drinking water, especially those induced by existing infrastructure. One such threat has been identified as a group of waterborne pathogens known as opportunistic premise plumbing pathogens (OPPPs). OPPPs exhibit thermal-tolerance, disinfectant-resistance, and growth under oligotrophic conditions, which make water distribution systems favorable habitats for their survival. *Legionella pneumophila* is one of the most notorious OPPPs and is presently one of the most threatening waterborne pathogens, particularly in developed countries. Reported cases of Legionnaires' disease have increased dramatically since the turn of the century. It is clear that this is a serious public health concern that could be better mitigated by improved forms of detection of the pathogen before human exposure. Biosensors have been identified as a potential source of on-site monitoring for pathogenic threats. This thesis focuses on optimizing the application of DNA as a bioreceptor for detection of *L. pneumophila*. The first chapter provides information on existing forms of detection for monitoring waterborne pathogens, OPPPs, DNA-based biosensors, as well as DNA quantification and hybridization. There is a discussion on current gaps and challenges with existing methods of waterborne pathogenic monitoring and the review of numerous electrochemical DNA-based biosensing schemes developed specifically for pathogen detection. The second chapter explains two different methodologies employing the Qubit fluorometer developed for selective quantification of DNA that isolates and measures single-stranded DNA (ssDNA) and double-stranded DNA (dsDNA). The first method allows for accurate quantification of DNA probes that contain both ssDNA and dsDNA, such as hairpins. The next method provides a means to quantify dsDNA present post-hybridization, when in solution with excess unhybridized ssDNA. These methodologies prove important to measure the

number of probe copies in solution and the hybridization efficiency of a DNA probe. The third chapter compares hybridization efficiencies capable for linear (LSP) and dangling-ended hairpin (Key) DNA probes, both in solution and immobilized on a magnetic microparticle surface. In the third chapter, data is provided that displays linear DNA probes that have higher affinity for the target DNA sequence than dangling-ended hairpin probes, when hybridized in a solution of ultrapure water. Ultimately, when hybridization efficiency is quantified again with the probes immobilized, there is not a significant difference in hybridization between the two different structures. The final chapter covers conclusions, engineering significance, and recommendations for future work. Through this research, more information about the application for DNA probes in biosensors was collected. The linear DNA probes observed higher sensitivity than the hairpin probes for detection in solutions absent of salt. However after immobilization, probe structure did not yield a significant change in sensitivity for detection, in a buffered saline solution. These results can be used to further optimize DNA-based biosensors.

CHAPTER 1. GENERAL INTRODUCTION

Maintaining safe, potable water is vital to the proliferation of every civilization across the globe (1). Between the obvious threats, such as industrial pollution, and the pervasive, more recently acknowledged threats, such as pharmaceuticals, personal care products, and opportunistic pathogens, water quality is both a pertinent and growing field of scientific study (2–5). To protect public health, known threats to the quality of drinking water need to be monitored in real-time. Monitoring for dangerous pollutants allows for rapid response to contamination, preventing the spread of pollution while protecting public health and water security (6–8).

Potable water quality is dynamic and changes depending on geographic location, infrastructure, water age, and countless other factors (9, 10). Even if water has undergone treatment, the degradation of quality can occur while contained and transported in water distribution systems. As witnessed in Flint, Michigan, infrastructure and source water can be detrimental on drinking water, and fluctuations in water chemistry can have immense influence on pathogen abundance. If conditions are favorable, water distribution systems can be a conducive habitat for dangerous pathogens (11). Opportunistic premise plumbing pathogens (OPPPs) are robust microorganisms capable of thriving in plumbing systems (12). Illnesses induced by these pathogens are on the rise and will continue to increase without a timely mode of detection (13). Although water provided through public water systems receives treatment, upholding the quality of potable water is not the sole responsibility of the municipality. Property owners carry the responsibility of ensuring their premise plumbing does not deteriorate the water quality prior to reaching the tap (14). Simple management practices, such as increasing the temperature of hot water heaters, removal of any faucets or showerheads that induce

aerosolization, routinely disinfecting showerheads, application of microbial filters at faucets and showerheads, and flushing pipes after periods of stagnation, have been noted as means to mitigate OPPPs or lower exposure, yet depending on the ownership of the property, these might not even be possible for an individual (12, 15, 16). If an individual is concerned with the quality of their potable water, the Environmental Protection Agency (EPA) suggests contacting the local health department or a state certified laboratory for testing (17). However, this does not provide real-time monitoring for threats that could accumulate over time.

To protect public health and ensure adequate water quality within premise plumbing, monitoring devices need to be integrated within water distribution systems. Biosensors have been identified as a means of highly specific detection or quantification that can support *in situ* monitoring, distinguishing biosensors as a propitious solution to this issue (18). This research focuses on the optimization of biorecognition via DNA hybridization to determine DNA structures most suitable for detection of pathogens in premise plumbing water.

Methods of Detection for Waterborne Pathogens

Common forms of waterborne pathogen detection involve cultural, phenotypic, or molecular techniques (13). Cultural methods involve inoculation of a plate prepared with media to encourage the multiplication of microorganisms till observable colonies have formed. Cultured colonies can be counted to determine the severity of the microbiological threat (19). Unfortunately, multiple waterborne pathogens are capable of entering a viable but non-culturable (VBNC) state, decreasing the applicability of conventional culture methods (20, 21). Furthermore, conventional culture methods need days to produce results (22). Comparatively, phenotypic and molecular methods have faster response times, and thus, prove to be powerful tools for swift risk assessment. Phenotypic assays employ detection of physiological characteristics specific to the targeted pathogen, such as immunoassays that utilize antibody-

antigen interactions (13). These immunological techniques exist in a variety of configurations, such as immunofluorescence assays and enzyme-linked immunosorbance assays (ELISA), which employ antibodies conjugated with fluorescent or enzymatic labels for signal production (23, 24). Yet, constraints associated with antibody-based methodologies have been reported, such as low sensitivity, the need for pre-treatment, and cross-reactivity with other close antigens (22, 25). Since some opportunistic pathogens have the ability to survive inside amoebae, pre-treatment steps, such as cell lysis, can be pivotal for target antigens that exist intracellularly (26, 27). Molecular methods generally involve identification of biomarkers that contain specific genetic information. Many of these techniques, such as fluorescence *in situ* hybridization (FISH), DNA microarrays, and types of polymerase chain reaction (PCR), are reliant on detection via hybridization events with target sequences (13). FISH is a method that employs rRNA probes containing fluorescent labels (25). These methods can detect intracellular targets but have been criticized for low sensitivity, arduous procedures, and the influence of signal production based on physiological conditions of the targeted organism (28). Other molecular methods require the pre-treatment step of DNA extraction (29). DNA microarrays rely on hybridization with DNA probes that are immobilized to capture and isolate a target sequence. Although a potential tool for multiplexed detection, DNA microarrays have also been criticized for their lack of sensitivity (28, 30). PCR, and the multiple variations such as mPCR and qPCR, utilizes primers that amplify a target sequence of DNA. As a result of the amplification step, PCR is a sensitive methodology, yet it is challenged by the need for specific primers and reaction conditions. Improvements in terms of sensitivity can be made by combining techniques; methods that rely on hybridization for detection, such as DNA microarrays, have been combined with PCR to amplify target DNA sequences and increase sensitivity of the method (25, 29). However, all previously described

methods experience constraints based on time, representative sampling, trained personnel, or application of specialized equipment suited for a laboratory setting (13, 31). Even with OPPPs a prevalent origin of disease in the potable water of developed countries (32–34), there is presently no consensus on strategies for monitoring OPPPs. As the threat of OPPPs continue to grow, so does the need for dependable monitoring methodologies (13), and biosensors have been noted as a potential solution for continuous, on-site monitoring that permit faster detection without the need for trained personnel (35, 36).

Opportunistic Premise Plumbing Pathogens

Opportunistic premise plumbing pathogens (OPPPs) are microorganisms that have adapted to growth and persistence in the premise plumbing that stores and supplies potable water (12). OPPPs share a number of characteristics that contribute to their proliferation in water plumbing systems, including thermal-tolerance, disinfectant-resistance, and growth under oligotrophic conditions. As a result of the thermal-tolerance, even water that passes through hot water heaters is susceptible to the presence of OPPPs (27). Since OPPPs are relatively chlorine resistant, they proliferate while other competitors for nutrients are eradicated by the disinfectant (12). In addition, OPPPs are known for displaying resistance to amoeba phagocytosis, meaning they can survive, and even proliferate, within the confines of other microorganisms. Other factors that connect OPPP presence to infrastructure include water age and characteristics of the piping material (37). Premise plumbing supplied on the outer periphery of the distribution system experiences longer residence times. This can mean lower concentrations of residual chlorine for control of pathogens (9). In addition, periods of stagnation can lead to increased growth of biofilms and dangerous microbiota. Therefore, buildings that experience intermittent flow and routine periods of stagnation are particularly susceptible to elevated concentrations of pathogens (12). Age of the piping material can be another influencing factor on the water chemistry in

premise plumbing. For example, the increasing age of pipes containing iron has been noted to correlate with corrosion that leads to increased release of iron (38). Iron corrosion can induce chlorine degradation, and iron can act as a nutrient source for pathogens (39). From the first deadly outbreak in 1976 in Philadelphia, Pennsylvania to the outbreak in Flint, Michigan nearly 40 years later, *L. pneumophila* is one of the most notorious OPPPs and is presently one of the most threatening waterborne pathogens, particularly in developed countries (40). The annual cost of infections in the United States associated with *Legionella* spp. alone has been estimated to be over 430 million dollars (12). According to the Centers for Disease Control (CDC) and the National Notifiable Diseases Surveillance System (NNDSS), since the turn of the century, reported cases of Legionnaires' disease have increased over five times, as seen in Fig. 1.1.

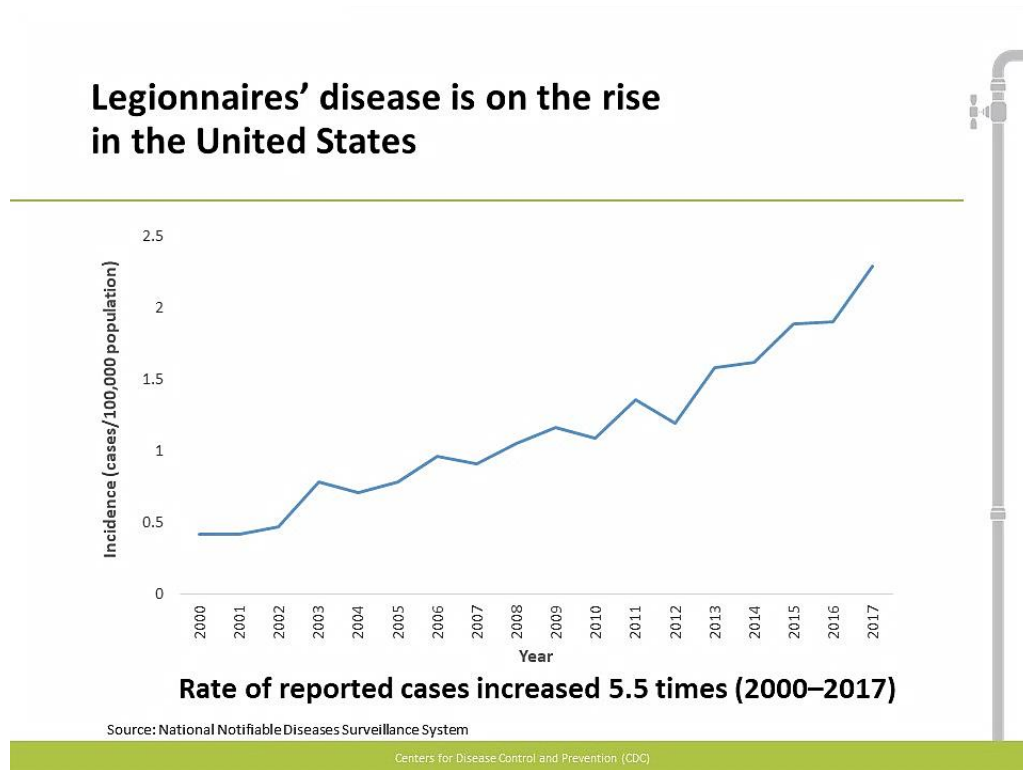


Figure 1.1. Reported cases of Legionnaires' disease since the beginning of the 21st century, made available by the CDC and NNDSS (41).

Although it is unclear whether the dramatic increase in the occurrence of Legionnaires' disease is due to an increasing immunologically susceptible population, increasing awareness of testing, or increasing prevalence of *Legionella*, Legionnaires' disease is clearly a serious public health concern that could benefit from improved forms of detection (41).

As a preliminary evaluation of the extent of OPPP contamination in premise plumbing, I collected potable water at a public school located in Sevier County, Tennessee. The water samples were screened for five bacterial species and three genera that have been identified as OPPPs. The original building was constructed in the early 20th century. Since then, additional construction has increased the size of the school. The specific history of the school's premise plumbing and infrastructure was not readily available, but water samples were collected throughout the school. Water samples were collected from taps at the front, middle, and back of the school, with the building's age increasing from front to back. To screen for pathogens, DNA primers were used to amplify target sequences via PCR. The amplified sample was then visualized by gel electrophoresis to determine the absence or presence of the targeted DNA sequence. The presence or absence of the target pathogens at the sampling location is shown in Table 1.1. Targeted genes, primer sequences, sequence specific PCR protocols, and sequence references are provided in Table A.1. Although most faucets in the school did not appear to be contaminated with pathogens, the results did confirm the presence of *Mycobacterium* spp. and *Legionella* spp. *Mycobacterium* spp. was found at faucets at the front, middle, and back, while *Legionella* spp. was only found in the back of the school. This case study reveals the presence of potential pathogenic threats to public health, and the need for improved forms of detection, especially at locations largely visited by populations of individuals with compromised immune systems (12), such as nursing homes and hospitals.

Table 1.1. OPPPs screened at various locations in the school via PCR and electrophoresis gels. Red means the presence of the listed pathogen; otherwise, black means it was not detected.

Pathogen	Front	Middle	Back
<i>Acinetobacter baumannii</i>			
<i>Aeromonas hydrophila</i>			
<i>Legionella</i> spp.			
<i>Legionella pneumophila</i>			
<i>Methylobacterium</i> spp.			
<i>Mycobacterium</i> spp.			
<i>Mycobacterium avium</i>			
<i>Pseudomonas aeruginosa</i>			

Biosensors

According to the International Union of Pure and Applied Chemistry, a biosensor is defined as an integrated receptor-transducer device, which is capable of providing selective quantitative or semi-quantitative analytical information using a biological recognition element. Biosensors have broad applicability and flexibility and can be engineered to identify a plethora of analytes, including both organic and inorganic targets (42). These devices have undergone successful implementation in environmental monitoring, food safety, and biomedicine (43, 44). Biosensors have even been developed for identifying and measuring specific microbial species (18), making these devices ideal for detection of OPPPs. Depicted in Fig. 1.2, a biosensor is composed of two major components: a bioreceptor and a transducer. A multiplicity of combinations of bioreceptor and transducer exist, depending on the target analyte. Providing a holistic list of bioreceptors and transducers is a difficult task, considering the realm of biosensing is still growing and evolving. Essentially, a bioreceptor is any organic body that detects any particular analyte from the medium of interest, while remaining unresponsive towards other

potentially interfering species; a transducer is the mechanism that converts the response of the bioreceptor into a measurable signal (45).

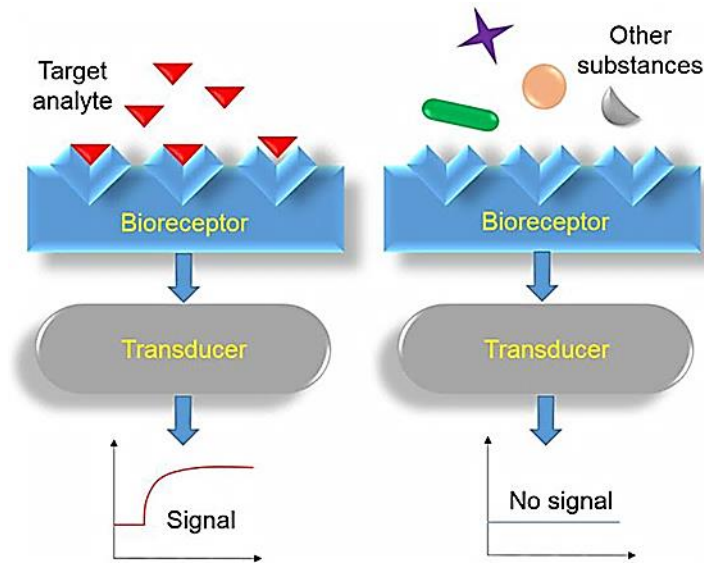


Figure 1.2. Diagram of the two major components of a biosensor (46).

When selecting bioreceptor and transduction elements, a plethora of factors must be considered, including specificity, sensitivity, portability, and affordability, among others (47). Commonly utilized bioreceptors include whole cells, phages, enzymes, antibodies, and nucleic acids (24). When comparing the commonly employed bioreceptors, nucleic acids appear to have multiple strengths. DNA-based biosensors are simple, cost-effective, and fast (30). Diverse immobilization strategies exist for nucleic acids that exhibit stability over long periods of time (48). Unlike other bioreceptors, nucleic acid probes can be produced via chemical synthesis and regenerated for reuse (22, 49). Nucleic acids also hold the potential for reagentless and label-free detection, removing the need for sacrificial substrates (50). Transduction elements often involve either optical or electrical responses that allow for detection of the target (51). Two broad forms of signal transduction include electrochemical and optical techniques. Even though proven to be sensitive methods, optical techniques, such as spectrometry, typically require expensive and large equipment that are better suited for a laboratory setting. For electrochemical techniques,

there is an ease of miniaturization for electrode systems and an ability to work with turbid samples (24, 30, 52). Acknowledging the functionality of this detection scheme, various studies have been conducted in the field of electrochemical DNA-based biosensors for pathogen quantification and detection (53). An immense variety of research endeavors have focused on the implementation of DNA for electrochemical biosensing; to briefly describe trends, advances, and difficulties in this area of biosensor development, a small pool of relevant biosensors for pathogen detection has been selected for discussion.

Sandwich DNA hybridization is a common strategy for electrochemical DNA-biosensors, which involves two separate hybridization events to isolate target DNA with a capture probe that is immobilized on an electrode surface and a signal probe that has been functionalized to have a quantifiable electrochemical response (54). An example of a sandwich-based biosensor is depicted in Fig. 1.3. In one DNA sandwich detection scheme by Wang et al., a capture probe immobilized on a gold surface was utilized to bind with target DNA (55).

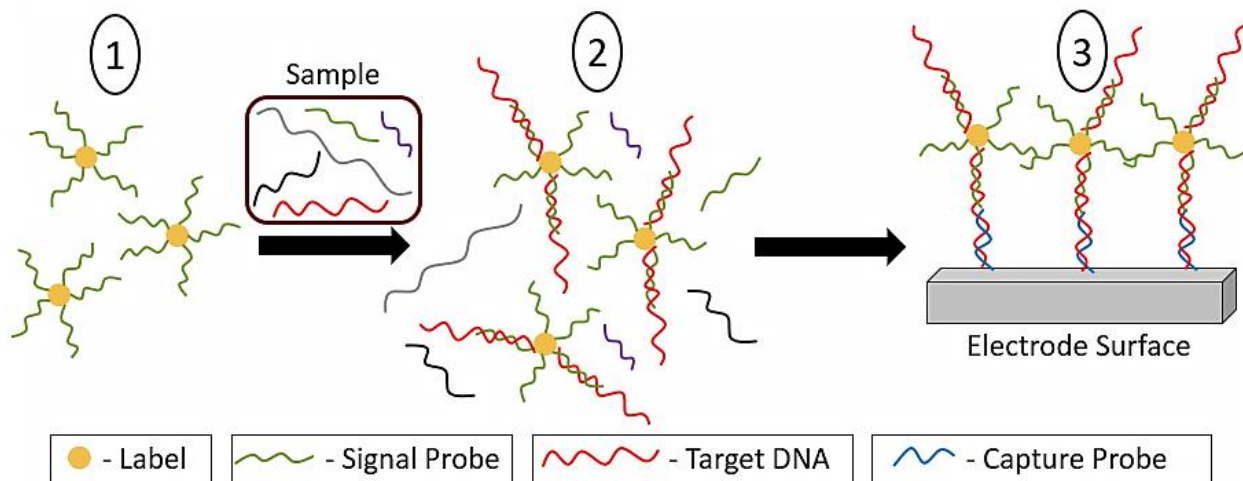


Figure 1.3. Example of a sandwich DNA hybridization strategy for biosensing detection. Adapted from (56).

This was followed by a secondary hybridization event that occurred between the target and immobilized DNA with a signal probe containing biotin. Conjugates composed of streptavidin, gold nanoparticles, and 6-ferrocenylhexanethiol attached to the biotinylated signal probe. Using the redox reaction of ferrocene at the electrode surface, this sensing scheme was capable of quantifying target DNA voltammetrically. This DNA-based biosensor displays the applicability of using DNA to not only isolate targets, but also label them for signal production. In a different study, a PCR-coupled electrochemical biosensor was designed for quantification of *L. pneumophila* (57). The biosensor employed a sandwich-based DNA assay with the target strand hybridized between a signal and a capture probe. The first hybridization event occurred between the target sequence and biotinylated signal probe. Then, the hybridized target and signal probe were exposed to the immobilized hairpin capture probe. After both hybridization events, the sample was exposed to alkaline phosphatase enzymes conjugated to streptavidin. The enzymatic response to a substrate was quantified via differential pulse voltammetry (DPV). This sensing mechanism displays the functionality of using DNA as a bioreceptor, yet the incorporation of PCR reveals the need to carry out sample preparation to generate a larger signal for detection. Another electrochemical DNA-based biosensor that incorporates ferrocene was developed to target *Legionella* DNA by Rai et al. (58). Unlike the previously discussed schemes, this biosensor relied on only one hybridization event between the immobilized hairpin capture probe functionalized with ferrocene and the target DNA. The presence or absence of ferrocene at the electrode surface was utilized to determine hybridization with the target DNA via DPV. Although this biosensing mechanism boasts label-free detection, it still required the application of a sacrificial redox reagent for electrochemical detection. In fact, each aforementioned biosensor required the use of sacrificial reagents or signal probes that could not be recovered or

reused, which could be a limiting factor in the lifecycle of the sensor, increasing the cost and complexity of the test. Regardless, these biosensors point to the diversity and novelty possible in the realm of DNA-based electrochemical detection, as well as the incentive to create a functional, affordable system with regenerative or reusable signal production.

The progression of microfluidics, microfabrication, and nanotechnology has also had a direct impact on the architecture of biosensors. With major motivations for biosensors to become more sensitive and functional, research has proven the importance of including new materials to improve sensitivity and reusability of biosensors (59). In one study, streptavidin coated magnetic beads were utilized for the development of a microarray for multiple oligonucleotides. A major noted advantage for the application of the magnetic particles was the increase in sensitivity due to the ability to wash away other potential sources of cross-reactivity (60). Another biosensing system enlisted the power of magnetic beads to isolate an *E. coli* specific gene. Due to the complex nature of real samples, magnetic separation was noted as an effective means of target isolation. For this sensing scheme, daunomycin was utilized as a hybridization indicator, still requiring the application of a sacrificial reagent. However, this study achieved a detection limit of 50 cells/mL without pretreatment (61). In a study by Hu et al., the functionality of magnetic separation was also displayed in the ability to recover and reuse magnetic particles functionalized with DNA (62). The schematic presented in Fig. 1.4 displays one potential microfluidic design for the incorporation of magnetic particles in an electrochemical DNA-based biosensor.

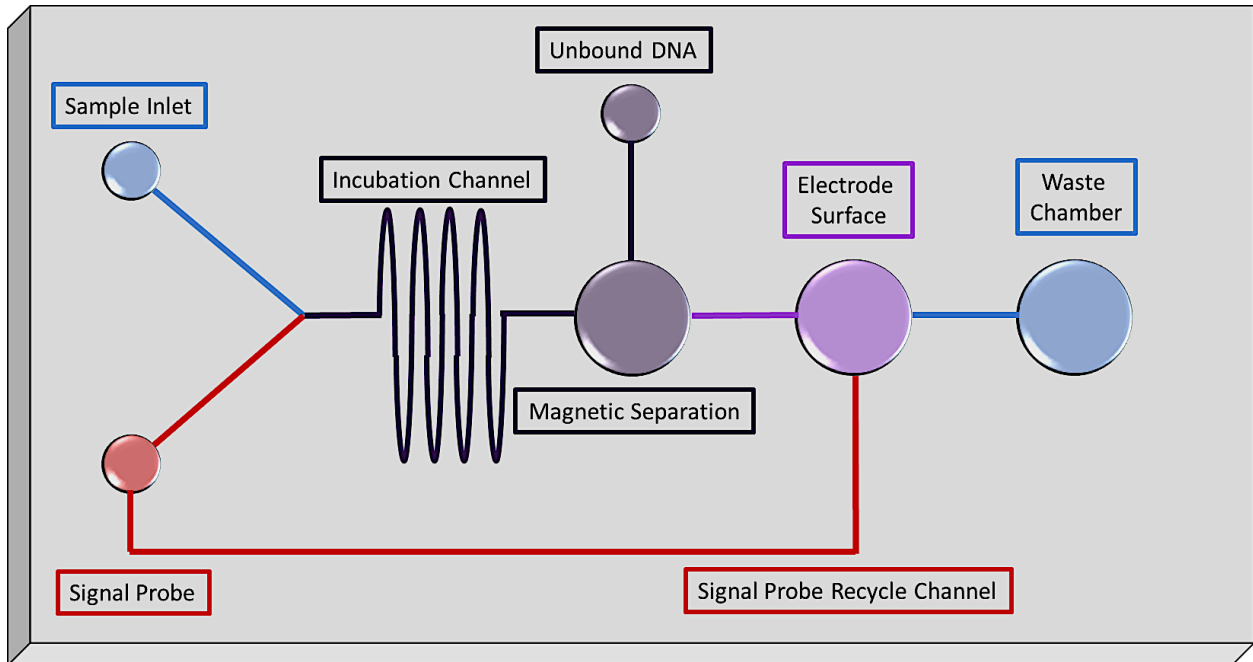


Figure 1.4. Schematic of a potential microfluidic device for an electrochemical DNA-based biosensor. Adapted from (63).

There has even been described the unique application of streptavidin coated magnetic beads through integration of the particles with primers for application with isothermal PCR. The reverse primers were attached to the magnetic beads and the forward primers were tagged with gold nanoparticles, which were used for the electrochemical detection via chronoamperometry (64). These sensors provide just a few examples of how advances in materials are driving innovation and improving the realm of biosensors.

It is important to note that as new materials are developed and being applied to improve biosensor performance, advances in biology and DNA hybridization are also improving the selectivity and sensitivity of DNA bioreceptors. Nucleic acids have manipulative structures that can be engineered into a variety of structures that consequently can alter hybridization affinity. In multiple biosensors, the application of the hairpin DNA structure has been described not only as a method to aid in label-free detection, but also increase the selectivity of hybridization (58,

65). In one study, a biosensing scheme integrated triplex-forming oligonucleotides into a tetrahedral DNA nanostructure that would bind to the base of the tetrahedral structure in the presence of the target DNA (66). As similarly reported in other biosensor studies, the switching DNA contained a redox reporter, yet the unique DNA nanostructure aided in suppressing background noise. Furthermore, the bioreceptor exhibited a rapid response time of approximately 35 minutes and simple regeneration through application of a buffer. In a different study, DNA nanomaterial was once again exploited for electrochemical detection by Y-shaped DNA composed of three different sequences (67). In the presence of the target sequence, the Y-shape was disrupted, inducing a chain of hybridization reactions. The substantial structural changes that occurred as a result of the hybridization event was quantifiable through cyclic voltammetry (CV) and electrochemical impedance spectroscopy (EIS). Through the aforementioned selected examples of DNA-based electrochemical biosensors, it is clear that even this specific niche of biosensors has wide range and diversity of designs, compositions, and materials.

DNA Quantification

As mentioned previously, forms of DNA quantification are applicable methodology for determining the threat of *L. pneumophila* and other pathogens that cannot be readily cultured (13). DNA quantification is often the precursor to more complex DNA analysis, such as DNA sequencing, and is necessary for the process of developing and optimizing the use of DNA as a bioreceptor. Two of the most common forms of measuring DNA concentration in a laboratory setting are spectrophotometry and fluorometry (68, 69). Spectrophotometry can be used to quantify the concentration of DNA based on Beer-Lambert's law (70). When using spectrophotometry, the amount of light absorbed at 260 nm is proportional to the amount of DNA present, while the ratio of absorbances for 260/280 and 260/230 nm can be used to determine sample purity (71). Fluorometric methods require the application of dyes or

fluorochromes, which fluoresce corresponding to concentrations of DNA (72).

Spectrophotometry methods utilize small sample sizes and has the added benefit of no additional reagents (73, 74). However, spectrophotometry does not provide specificity for differentiating single-stranded DNA (ssDNA) and double-stranded DNA (dsDNA). Comparatively, fluorometric techniques provide more sensitive and selective detection for DNA quantification (69). Fluorochromes are capable of achieving quantification of concentrations lower than that of spectrophotometric means, as well as selective binding to ssDNA or dsDNA (75). The ability to measure low concentrations of DNA can be of utmost importance, especially when working with samples that contain low concentrations of biomass, such as samples from premise plumbing (13). qPCR involves the amplification of target DNA alongside fluorometric techniques for quantification of specific DNA sequences. These methods can involve the incorporation of dyes or functionalized DNA probes. Although a sensitive method for DNA quantification, the methodology requires application of specific primers, can be influenced by sample conditions, and does not differentiate between ssDNA and dsDNA (71).

Two instruments commonly found in laboratories that conduct spectrophotometric and fluorometric techniques for DNA quantification are the NanoDrop™ Spectrophotometer and Qubit™ Fluorometer, respectively (68). Comparative studies have claimed the Qubit fluorometer to be more sensitive than the NanoDrop spectrophotometer for quantifying DNA (76, 77). In addition to sensitivity, selectively differentiating DNA structure can be pivotal for quantifying DNA in a sample containing both ssDNA and dsDNA, or even quantifying concentrations of DNA that exist as a complex structure. Although ssDNA and dsDNA have different extinction coefficients (78), both forms still absorb light at 260 nm. Therefore, spectrophotometric techniques struggle with reliable quantification that can detail structural intricacies. Despite

being more sensitive and selective, it has been reported that Qubit assays for dsDNA measurement still detect 2–10% of pure ssDNA for the majority of the quantifiable range (79).

Although the NanoDrop cannot be readily used for measurements of DNA that contain both ssDNA and dsDNA, there have been attempts to add sample treatment steps in conjunction with the spectrophotometric measurement to produce more dependable quantification. In a study by Nwokeoji et al., a spectrophotometric method for accurate quantification of nucleic acids was developed through determination of hypochromicity by comparing absorbance of nondenatured and denatured sequences (80). A variety of methods exist to denature DNA, including heat exposure, sonication, raising the pH, and increasing the salt concentration, among others (81). To ensure prolonged denaturation of the nucleic acids, the samples were exposed to dimethyl sulfoxide (DMSO) and thermal treatment. Through this method, more accurate extinction coefficients were produced, ultimately yielding more accurate measurements. In addition, the hyperchromic effect was utilized to calibrate changes in absorbance with respect to the percentage of double-stranded nucleic acids, allowing for the specific quantification of double-stranded and single-stranded structures in solutions containing both. The accuracy of the methodology was displayed in the ability to quantify the relative proportion and concentration of standards containing 25% and 50% double-stranded RNA (dsRNA), as 24.4% and 49.1% respectively. Although the method is described as applicable to dsDNA, the lowest relative proportion and concentration for dsRNA reported was 15.2% (175.7 ng/ μ L); thus, this method might be best suited for situations in which there is an excess of nucleic acids available for quantification. Accurate, selective quantification of different DNA structures can be particularly crucial when ssDNA is present with complementary sequences, potentially yielding hybridized duplexes and mixed solutions of ssDNA and dsDNA. Fluorometry has been utilized to quantify

hybridization via labeling DNA probes with fluorophores or quenchers that either fluoresce or stop fluorescing after hybridizing with the complementary strand. Consequently, the change in fluorescence can be used to quantify the hybridization event (82). Detection of hybridization via functionalized DNA probes with fluorescent labels has been used in a variety of studies (83–86). However, synthesizing labeled oligonucleotides is an expensive process (87, 88). In a sample containing unknown ratios of hybridized duplexes, DNA probes, and complementary sequences, it is currently not possible to discern how much of the signal is generated by ssDNA or dsDNA, without additional sample treatment or functionalization.

DNA Hybridization

At the crux of a DNA-based biosensor is DNA hybridization. Understanding hybridization is pivotal to the success of implementing DNA as a bioreceptor. Factors influencing hybridization and stability of DNA duplexes include temperature, solution composition, and sequence composition, among others (89). As the field of DNA-based biosensors has grown, there has been diverse application of DNA in different structural forms. Understanding how structural differences of the DNA influence binding affinity is beneficial to the application of nucleic acids in biosensors. DNA can take a variety of forms and exist in diverse structures (90). DNA exhibiting some of the structures seen in Fig. 1.5, have been applied to DNA detection and quantification technologies, due to the more selective or sensitive hybridization that these structures provide (65, 91). For example, a vast amount of studies has been conducted utilizing the classic hairpin structure, as a result of its applicability and functionality in the realm of biosensors (58, 92, 93). Due to the self-annealing segment that shields the sequence, hairpins have been shown to increase the selectivity of a binding event. The activation energy necessary to open the hairpin loop and hybridize shows to be more selective compared to hybridization with linear DNA probes (94).

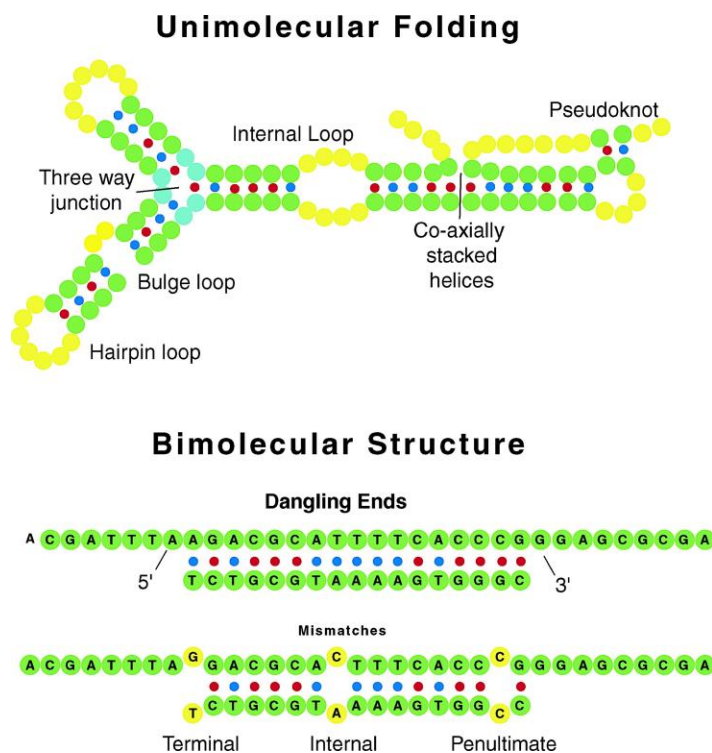


Figure 1.5. Examples of DNA motifs that are available through intramolecular and intermolecular interactions (89).

The potential influence on hybridization efficiency of hairpin structures with dangling ends has also been reviewed. One study found that immobilized DNA probes, with a dangling end, yielded better rates of hybridization compared to other linear DNA probes (83). The underlying theory behind the improved hybridization efficiency is partially a result of the additional stacking interactions with the structured probe at the dangling end, which yields greater stability and quicker reaction kinetics, compared to linear probes (91).

In the context of a biosensor, hybridization commonly involves immobilized DNA probes. Hybridization with surface-tethered DNA introduces other factors, such as probe density and surface geometry (95). The thermodynamics of solution-phase hybridization can be sufficiently predicted via the nearest-neighbor model (90). However, nucleic acid hybridization at an interface involves additional complexities, when compared to hybridization in solution

(95). With major motivation for biosensors to become more sensitive and functional, research has shown the importance of including new materials to improve the functionality of biosensors. More studies are necessary to develop an improved understanding of how DNA structure influences hybridization, especially when comparing solution- and surface-phase hybridization. Since a multiplicity of conditions influence hybridization, these conditions and limitations should be explored further as means to fully optimize and improve existing DNA-based biosensors for pathogen detection.

Scope of Research

Based on the reviewed literature, there is a critical need for more development and optimization of methods focused on the detection and quantification of pathogenic DNA to protect water quality and public health. Electrochemical DNA-based biosensors have the potential to fill the need for *in situ* monitoring of water quality in premise plumbing. A vast amount of research has proven effective integration of nucleic acids as a bioreceptor, while employing different DNA structures and microfabricated materials. However, there has not been much research on the hairpin dangling structure as a DNA probe, particularly immobilized on a particle surface.

This M.S. research assessed the feasibility of DNA composed of different structures as signal probes for application in a biosensor. Through evaluation of hybridization both in solution and immobilized on a magnetic particle, a more holistic picture of how immobilization influences DNA hybridization was obtained and consequently its impact on biosensing application.

The objectives of this M.S. research were to:

1. Establish methods for accurate quantification of ssDNA probes and dsDNA after hybridization using the Qubit fluorometer methodology, and

2. Evaluate the effect of structure on DNA hybridization in solution and immobilized on a particle surface for optimized detection of *L. pneumophila*.

References

1. Brookes, J.D. and Carey, C.C. (2015) Goal 6—Rising to the Challenge: Enabling Access to Clean and Safe Water Globally. *UN Chron.*
2. Fawell, J. and Nieuwenhuijsen, M.J. (2003) Contaminants in drinking water. *Br. Med. Bull.*, **68**, 199–208.
3. Fawell, J. (2015) Emerging contaminants, source water quality and the role of standards. *Water Pract. Technol.*, **10**, 432–437.
4. Richardson, S.D. and Ternes, T.A. (2018) Water Analysis: Emerging Contaminants and Current Issues. *Anal. Chem.*, **90**, 398–428.
5. Hull, N.M., Ling, F., Pinto, A.J., Albertsen, M., Jang, H.G., Hong, P.Y., Konstantinidis, K.T., LeChevallier, M., Colwell, R.R. and Liu, W.T. (2019) Drinking Water Microbiome Project: Is it Time? *Trends Microbiol.*, **27**, 670–677.
6. Lambrou, T.P., Anastasiou, C.C., Panayiotou, C.G. and Polycarpou, M.M. (2014) A low-cost sensor network for real-time monitoring and contamination detection in drinking water distribution systems. *IEEE Sens. J.*, **14**, 2765–2772.
7. Vijayakumar, N. and Ramya, R. (2015) The real time monitoring of water quality in IoT environment. In *ICIIECS 2015 - 2015 IEEE International Conference on Innovations in Information, Embedded and Communication Systems*. IEEE, pp. 1–5.
8. Capodaglio, A.G., Callegari, A. and Molognoni, D. (2016) Online monitoring of priority and dangerous pollutants in natural and urban waters: A state-of-the-art review. *Manag. Environ. Qual. An Int. J.*, **27**, 507–536.
9. Turgeon, S., Rodriguez, M.J., Thériault, M. and Levallois, P. (2004) Perception of drinking water in the Quebec City region (Canada): The influence of water quality and consumer location in the distribution system. *J. Environ. Manage.*, **70**, 363–373.
10. Wang, H., Masters, S., Edwards, M.A., Falkinham, J.O. and Pruden, A. (2014) Effect of disinfectant, water age, and pipe materials on bacterial and eukaryotic community structure in drinking water biofilm. *Environ. Sci. Technol.*, **48**, 1426–1435.
11. Liu, G., Zhang, Y., Knibbe, W.J., Feng, C., Liu, W., Medema, G. and van der Meer, W. (2017) Potential impacts of changing supply-water quality on drinking water distribution: A review. *Water Res.*, **116**, 135–148.

12. Falkinham, J.O., Pruden, A. and Edwards, M. (2015) Opportunistic Premise Plumbing Pathogens: Increasingly Important Pathogens in Drinking Water. 10.3390/pathogens4020373.
13. Wang, H., Bédard, E., Prévost, M., Camper, A.K., Hill, V.R. and Pruden, A. (2017) Methodological approaches for monitoring opportunistic pathogens in premise plumbing: A review. *Water Res.*, **117**, 68–86.
14. National Research Council. (2006) 8 Alternatives for Premise Plumbing. In *Drinking Water Distribution Systems: Assessing and Reducing Risks*. The National Academies Press, Washington, DC, pp. 316–392.
15. Hilborn, E.D., Arduino, M.J., Pruden, A. and Edwards, M.A. (2015) Review Epidemiology and Ecology of Opportunistic Premise Plumbing Pathogens: *Legionella pneumophila*, *Mycobacterium avium*, and *Pseudomonas aeruginosa*. *Environ. Health Perspect.*, **123**, 749–758.
16. Ling, F., Whitaker, R., LeChevallier, M.W. and Liu, W.T. (2018) Drinking water microbiome assembly induced by water stagnation. *ISME J.*, **12**, 1520–1531.
17. United States Environmental Protection Agency. (2005) Home Water Testing.
18. Zhao, X., Lin, C.W., Wang, J. and Oh, D.H. (2014) Advances in rapid detection methods for foodborne pathogens. *J. Microbiol. Biotechnol.*, **24**, 297–312.
19. De Boer, E. and Beumer, R.R. (1999) Methodology for detection and typing of foodborne microorganisms. *Int. J. Food Microbiol.*, **50**, 119–130.
20. Bédard, E., Charron, D., Lalancette, C., Déziel, E. and Prévost, M. (2014) Recovery of *Pseudomonas aeruginosa* culturability following copper- and chlorine-induced stress. *FEMS Microbiol. Lett.*, **356**, 226–234.
21. Dietersdorfer, E., Kirschner, A., Schrammel, B., Ohradanova-Repic, A., Stockinger, H., Sommer, R., Walochnik, J. and Cervero-Aragó, S. (2018) Starved viable but non-culturable (VBNC) *Legionella* strains can infect and replicate in amoebae and human macrophages. *Water Res.*, **141**, 428–438.
22. Zeng, L., Wang, L. and Hu, J. (2018) Current and Emerging Technologies for Rapid Detection of Pathogens. In *Biosensing Technologies for the Detection of Pathogens - A Prospective Way for Rapid Analysis*. pp. 5–19.
23. Rigonan, A.S., Mann, L. and Chonmaitree, T. (1998) Use of monoclonal antibodies to identify serotypes of enterovirus isolates. *J. Clin. Microbiol.*, **36**, 1877–1881.
24. Alahi, M.E.E. and Mukhopadhyay, S.C. (2017) Detection methodologies for pathogen and toxins: A review. *Sensors (Switzerland)*, **17**, 1–20.

25. Ramírez-Castillo, F.Y., Loera-Muro, A., Jacques, M., Garneau, P., Avelar-González, F.J., Harel, J. and Guerrero-Barrera, A.L. (2015) Waterborne pathogens: Detection methods and challenges. *Pathogens*, **4**, 307–334.
26. Rechnitzer, C., Williams, A., Wright, J.B., Dowsett, A.B., Milman, N. and Fitzgeorge, R.B. (1992) Demonstration of the intracellular production of tissue-destructive protease by *Legionella pneumophila* multiplying within guinea-pig and human alveolar macrophages. *J. Gen. Microbiol.*, **138**, 1671–1677.
27. Falkinham, J.O. (2015) Common Features of Opportunistic Premise Plumbing Pathogens. *Int. J. Environ. Res. Public Health*, **12**, 4533–4545.
28. Girones, R., Ferrús, M.A., Alonso, J.L., Rodriguez-Manzano, J., Calgua, B., de Abreu Corrêa, A., Hundesa, A., Carratala, A. and Bofill-Mas, S. (2010) Molecular detection of pathogens in water - The pros and cons of molecular techniques. *Water Res.*, **44**, 4325–4339.
29. Call, D.R. (2005) Challenges and opportunities for pathogen detection using DNA microarrays. *Crit. Rev. Microbiol.*, **31**, 91–99.
30. Velusamy, V., Arshak, K., Korostynska, O., Oliwa, K. and Adley, C. (2010) An overview of foodborne pathogen detection: In the perspective of biosensors. *Biotechnol. Adv.*, **28**, 232–254.
31. Law, J.W.F., Mutalib, N.S.A., Chan, K.G. and Lee, L.H. (2014) Rapid methods for the detection of foodborne bacterial pathogens: Principles, applications, advantages and limitations. *Front. Microbiol.*, **5**, 1–19.
32. Anaissie, E.J., Penzak, S.R. and Dignani, M.C. (2002) The hospital water supply as a source of nosocomial infections: A plea for action. *Arch. Intern. Med.*, **162**, 1483–1492.
33. Craun, G.F., Brunkard, J.M., Yoder, J.S., Roberts, V.A., Carpenter, J., Wade, T., Calderon, R.L., Roberts, J.M., Beach, M.J. and Roy, S.L. (2010) Causes of outbreaks associated with drinking water in the United States from 1971 to 2006. *Clin. Microbiol. Rev.*, **23**, 507–528.
34. Hilborn, E.D., Wade, T.J., Hicks, L., Garrison, L., Carpenter, J., Adam, E., Mull, B., Yoder, J., Roberts, V. and Gargano, J.W. (2013) Surveillance for waterborne disease outbreaks associated with drinking water and other nonrecreational water - United States, 2009–2010. *Morb. Mortal. Wkly. Rep.*, **62**, 714–720.
35. Rahim, H.A., Zulkifli, S.N., Adilla, N., Subha, M., Rahim, R.A. and Zainal Abidin, H. (2017) Water Quality Monitoring using Wireless Sensor Network and Smartphone-based Applications: A Review. *Sensors & Transducers*, **209**, 1–11.
36. Rogers, K.R. and Gerlach, C.L. (1996) Environmental biosensors: A status report. *Environ. Sci. Technol.*, **30**.

37. Ortolano,G.A., McAlister,M.B., Angelbeck,J.A., Schaffer,J., Russell,R.L., Maynard,E. and Wenz,B. (2005) Hospital water point-of-use filtration: A complementary strategy to reduce the risk of nosocomial infection. *Am. J. Infect. Control*, **33**.
38. McNeill,L.S. and Edwards,M. (2001) Iron pipe corrosion in distribution systems. *J. Am. Water Work. Assoc.*, **93**, 88–100.
39. Schwake,D.O., Garner,E., Strom,O.R., Pruden,A. and Edwards,M.A. (2016) *Legionella* DNA Markers in Tap Water Coincident with a Spike in Legionnaires' Disease in Flint, MI. *Environ. Sci. Technol. Lett.*, **3**, 311–315.
40. Cotruvo,J.A., Purkiss,D., Hazan,S., Sidari,F.P., DeMarco,P. and LeChevallier,M. (2019) Managing *Legionella* and Other Pathogenic Microorganisms in Building Water Systems. *J. Am. Water Works Assoc.*, **111**, 54–59.
41. Centers for Disease Control and Prevention (2018) *Legionella*: History, Burden, and Trends.
42. Thévenot,D.R., Toth,K., Durst,R.A. and Wilson,G.S. (2001) Electrochemical biosensors: Recommended definitions and classification. *Biosens. Bioelectron.*, **16**, 121–131.
43. Baruah,S. and Dutta,J. (2009) Nanotechnology applications in pollution sensing and degradation in agriculture. *Environ. Chem. Lett.*, **7**, 191–204.
44. Huang,R., Xi,Z. and He,N. (2015) Applications of aptamers for chemistry analysis, medicine and food security. *Sci. China Chem.*, **58**, 1122–1130.
45. Ali,J., Najeeb,J., Asim Ali,M., Farhan Aslam,M. and Raza,A. (2017) Biosensors: Their Fundamentals, Designs, Types and Most Recent Impactful Applications: A Review. *J. Biosens. Bioelectron.*, **08**, 0–9.
46. Wang, Ronghui, Li,Y. (2016) Biosensors for Rapid Detection of Avian Influenza. In *Steps Forwards in Diagnosing and Controlling Influenza*.pp. 61–84.
47. Vanegas,D.C., Gomes,C.L., Cavallaro,N.D., Giraldo-Escobar,D. and McLamore,E.S. (2017) Emerging Biorecognition and Transduction Schemes for Rapid Detection of Pathogenic Bacteria in Food. *Compr. Rev. Food Sci. Food Saf.*, **16**, 1188–1205.
48. Nimse,S.B., Song,K., Sonawane,M.D., Sayyed,D.R. and Kim,T. (2014) Immobilization techniques for microarray: Challenges and applications. *Sensors (Switzerland)*, **14**, 22208–22229.
49. Goode,J.A., Rushworth,J.V.H. and Millner,P.A. (2015) Biosensor Regeneration: A Review of Common Techniques and Outcomes. *Langmuir*, **31**, 6267–6276.
50. Lucarelli,F., Tombelli,S., Minunni,M., Marrazza,G. and Mascini,M. (2008) Electrochemical and piezoelectric DNA biosensors for hybridisation detection. *Anal. Chim. Acta*, **609**, 139–159.

51. Bhalla,N., Jolly,P., Formisano,N. and Estrela,P. (2016) Introduction to biosensors. *Essays Biochem.*, **60**, 1–8.
52. Ahmed,A., Rushworth,J. V., Hirst,N.A. and Millner,P.A. (2014) Biosensors for Whole-Cell Bacterial Detection. *Clin. Microbiol. Rev.*, **27**, 631–646.
53. Liu,A., Wang,K., Weng,S., Lei,Y., Lin,L., Chen,W., Lin,X. and Chen,Y. (2012) Development of electrochemical DNA biosensors. *TrAC - Trends Anal. Chem.*, **37**, 101–111.
54. Rashid,J.I.A. and Yusof,N.A. (2017) The strategies of DNA immobilization and hybridization detection mechanism in the construction of electrochemical DNA sensor: A review. *Sens. Bio-Sensing Res.*, **16**, 19–31.
55. Wang,J., Li,J., Baca,A.J., Hu,J., Zhou,F., Yan,W. and Pang,D.W. (2003) Amplified voltammetric detection of DNA hybridization via oxidation of ferrocene caps on gold nanoparticle/streptavidin conjugates. *Anal. Chem.*, **75**, 3941–3945.
56. Zhang,J., Lao,R., Song,S., Yan,Z. and Fan,C. (2008) Design of an oligonucleotide-incorporated nonfouling surface and its application in electrochemical DNA sensors for highly sensitive and sequence-specific detection of target DNA. *Anal. Chem.*, **80**, 9029–9033.
57. Miranda-Castro,R., de-los-Santos-Álvarez,N., Lobo-Castañón,M.J., Miranda-Ordieres,A.J. and Tuñón-Blanco,P. (2009) PCR-coupled electrochemical sensing of *Legionella pneumophila*. *Biosens. Bioelectron.*, **24**, 2390–2396.
58. Rai,V., Nyine,Y.T., Hapuarachchi,H.C., Yap,H.M., Ng,L.C. and Toh,C.S. (2012) Electrochemically amplified molecular beacon biosensor for ultrasensitive DNA sequence-specific detection of *Legionella sp.* *Biosens. Bioelectron.*, **32**, 133–140.
59. Xu,Y. and Wang,E. (2012) Electrochemical biosensors based on magnetic micro/nano particles. *Electrochim. Acta*, **84**, 62–73.
60. Brandão,D., Liébana,S. and Pividori,M.I. (2015) Multiplexed detection of foodborne pathogens based on magnetic particles. *N. Biotechnol.*, **32**, 511–520.
61. Geng,P., Zhang,X., Teng,Y., Fu,Y., Xu,L., Xu,M., Jin,L. and Zhang,W. (2011) A DNA sequence-specific electrochemical biosensor based on alginate acid-coated cobalt magnetic beads for the detection of *E. coli*. *Biosens. Bioelectron.*, **26**, 3325–3330.
62. Hu,P., Cheng,Z.H., Yuan,F.L., Ling,J., Yu,L.L., Liang,R.F. and Jian,P.X. (2008) Magnetic particle-based sandwich sensor with DNA-modified carbon nanotubes as recognition elements for detection of DNA hybridization. *Anal. Chem.*, **80**, 1819–1823.
63. Hung, Tran Quang, Kim, Young Dong, Rao, B. Parvatheeswara, Kim,C. (2013) Novel Planar Hall Sensor for Biomedical Diagnosing Lab-on-a-Chip. In *State of the Art Biosensors - General Aspects*.pp. 197–239.

64. De La Escosura-Muñiz,A., Baptista-Pires,L., Serrano,L., Altet,L., Francino,O., Sánchez,A. and Merkoçi,A. (2016) Magnetic Bead/Gold Nanoparticle Double-Labeled Primers for Electrochemical Detection of Isothermal Amplified Leishmania DNA. *Small*, **12**, 205–213.
65. Miranda-Castro,R., De-los-Santos-Álvarez,N., Lobo-Castañón,M.J., Miranda-Ordieres,A.J. and Tuñón-Blanco,P. (2009) Structured nucleic acid probes for electrochemical devices. *Electroanalysis*, **21**, 2077–2090.
66. Yang,Y., Huang,Y. and Li,C. (2019) A reusable electrochemical sensor for one-step biosensing in complex media using triplex-forming oligonucleotide coupled DNA nanostructure. *Anal. Chim. Acta*, **1055**, 90–97.
67. Zhou,L., Wang,Y., Yang,C., Xu,H., Luo,J., Zhang,W., Tang,X., Yang,S., Fu,W., Chang,K., *et al.* (2019) A label-free electrochemical biosensor for microRNAs detection based on DNA nanomaterial by coupling with Y-shaped DNA structure and non-linear hybridization chain reaction. *Biosens. Bioelectron.*, **126**, 657–663.
68. Simbolo,M., Gottardi,M., Corbo,V., Fassan,M., Mafficini,A., Malpeli,G., Lawlor,R.T. and Scarpa,A. (2013) DNA Qualification Workflow for Next Generation Sequencing of Histopathological Samples. *PLoS One*, **8**.
69. Sedlackova,T., Repiska,G., Celec,P., Szemes,T. and Minarik,G. (2013) Fragmentation of DNA affects the accuracy of the DNA quantitation by the commonly used methods. *Biol. Proced. Online*, **15**, 1–8.
70. Leclerc,O., Fraisse,P.O., Labarraque,G., Oster,C., Pichaut,J.P., Baume,M., Jarraud,S., Fiscaro,P. and Vaslin-Reimann,S. (2013) Method development for genomic *Legionella pneumophila* DNA quantification by inductively coupled plasma mass spectrometry. *Anal. Biochem.*, **435**, 153–158.
71. Gryson,N. (2010) Effect of food processing on plant DNA degradation and PCR-based GMO analysis: A review. *Anal. Bioanal. Chem.*, **396**, 2003–2022.
72. Kumar,D., Panigrahi,M.K., Suryavanshi,M., Mehta,A. and Saikia,K.K. (2016) Quantification of DNA extracted from formalin fixed paraffin-embedded tissue comparison of three techniques: Effect on PCR efficiency. *J. Clin. Diagnostic Res.*, **10**, 3–5.
73. Desjardins,P. and Conklin,D. (2010) NanoDrop microvolume quantitation of nucleic acids. *J. Vis. Exp.*, 10.3791/2565.
74. O'Neill,M., McPartlin,J., Arthure,K., Riedel,S. and McMillan,N.D. (2011) Comparison of the TLDA with the nanodrop and the reference qubit system. *J. Phys. Conf. Ser.*, **307**.
75. Nielsen,K., Mogensen,H.S., Hedman,J., Niederstätter,H., Parson,W. and Morling,N. (2008) Comparison of five DNA quantification methods. *Forensic Sci. Int. Genet.*, **2**, 226–230.

76. Ponti,G., Maccaferri,M., Manfredini,M., Kaleci,S., Mandrioli,M., Pellacani,G., Ozben,T., Depenni,R., Bianchi,G., Pirola,G.M., *et al.* (2018) The value of fluorimetry (Qubit) and spectrophotometry (NanoDrop) in the quantification of cell-free DNA (cfDNA) in malignant melanoma and prostate cancer patients. *Clin. Chim. Acta*, **479**, 14–19.
77. Sarnecka,A.K., Nawrat,D., Piwowar,M., Ligeza,J., Swadźba,J. and Wójcik,P. (2019) DNA extraction from FFPE tissue samples – a comparison of three procedures. *Wspolczesna Onkol.*, **23**, 52–58.
78. He,H., Stein,E. V, DeRose,P. and Cole,K.D. (2017) Limitations of methods for measuring the concentration of human genomic DNA and oligonucleotide samples. **64**, 59–68.
79. Invitrogen (2016) Qubit dsDNA assay specificity in the presence of single-stranded DNA.
80. Nwokeoji,A.O., Kilby,P.M., Portwood,D.E. and Dickman,M.J. (2017) Accurate Quantification of Nucleic Acids Using Hypochromicity Measurements in Conjunction with UV Spectrophotometry. *Anal. Chem.*, **89**, 13567–13574.
81. Wang,X., Jeong Lim,H. and Son,A. (2014) Characterization of denaturation and renaturation of DNA for DNA hybridization. *Environ. Health Toxicol.*, **29**, 8.
82. Moreira,B.G., You,Y., Behlke,M.A. and Owczarzy,R. (2005) Effects of fluorescent dyes, quenchers, and dangling ends on DNA duplex stability. *Biochem. Biophys. Res. Commun.*, **327**, 473–484.
83. Riccelli,P. V, Merante,F., Leung,K.T., Bortolin,S., Zastawny,R.L., Janeczko,R. and Benight,A.S. (2001) Hybridization of single-stranded DNA targets to immobilized complementary DNA probes: comparison of hairpin versus linear capture probes. *Nucleic Acids Res.*, **29**, 996–1004.
84. Genot,A.J., Zhang,D.Y., Bath,J. and Turberfield,A.J. (2011) Remote toehold: A mechanism for flexible control of DNA hybridization kinetics. *J. Am. Chem. Soc.*, **133**, 2177–2182.
85. Chen,S.X. and Seelig,G. (2016) An Engineered Kinetic Amplification Mechanism for Single Nucleotide Variant Discrimination by DNA Hybridization Probes. *J. Am. Chem. Soc.*, **138**, 5076–5086.
86. Bui,H., Shah,S., Mokhtar,R., Song,T., Garg,S. and Reif,J. (2018) Localized DNA Hybridization Chain Reactions on DNA Origami. *ACS Nano*, **12**, 1146–1155.
87. Zhang,J.X., Fang,J.Z., Duan,W., Wu,L.R., Zhang,A.W., Dalchau,N., Yordanov,B., Petersen,R., Phillips,A. and Zhang,D.Y. (2018) Predicting DNA hybridization kinetics from sequence. *Nat. Chem.*, **10**, 91–98.
88. Kolpashchikov,D.M. (2019) Evolution of Hybridization Probes to DNA Machines and Robots. *Acc. Chem. Res.*, **52**, 1949–1956.

89. Wetmur, J.G. and Fresco, J. (1991) DNA probes: Applications of the Principles of Nucleic Acid Hybridization. *Crit. Rev. Biochem. Mol. Biol.*, **26**, 227–259.
90. SantaLucia, J. and Hicks, D. (2004) The Thermodynamics of DNA Structural Motifs. *Annu. Rev. Biophys. Biomol. Struct.*, **33**, 415–440.
91. Broude, N.E. (2002) Stem-loop oligonucleotides: A robust tool for molecular biology and biotechnology. *Trends Biotechnol.*, **20**, 249–256.
92. Xuan, F., Luo, X. and Hsing, I.M. (2012) Ultrasensitive solution-phase electrochemical molecular beacon-based DNA detection with signal amplification by exonuclease III-assisted target recycling. *Anal. Chem.*, **84**, 5216–5220.
93. Miranda-Castro, R., De-Los-Santos-Álvarez, P., Lobo-Castañón, M.J., Miranda-Ordieres, A.J. and Tuñón-Blanco, P. (2007) Hairpin-DNA probe for enzyme-amplified electrochemical detection of *Legionella pneumophila*. *Anal. Chem.*, **79**, 4050–4055.
94. Kolpashchikov, D.M. (2012) An Elegant Biosensor Molecular Beacon Probe: Challenges and Recent Solutions. *Scientifica (Cairo)*, **2012**, 1–17.
95. Ravan, H., Kashanian, S., Sanadgol, N., Badoei-Dalfard, A. and Karami, Z. (2014) Strategies for optimizing DNA hybridization on surfaces. *Anal. Biochem.*, **444**, 41–46.

CHAPTER 2. METHODS FOR ACCURATE QUANTIFICATION OF STRUCTURED DNA PROBES AND DOUBLE-STRANDED DNA AFTER HYBRIDIZATION USING THE QUBIT FLUOROMETER

Parker Dulin¹, Carmen Gomes², Kaoru Ikuma¹

¹Department of Civil, Construction and Environmental Engineering, Iowa State University, USA

²Department of Mechanical Engineering, Iowa State University, USA

Modified from a manuscript to be submitted to *MethodsX*

Abstract

DNA can exhibit a variety of structural forms and characteristics. As a result of their versatility and biocompatibility, DNA nanostructures have wide applicability in the field of biotechnology. However, in order to further study and optimize this functional tool, more sensitive and selective methods are needed for quantifying concentrations of DNA with complex structures. Existing methods of DNA quantification lack the selectivity necessary to accurately quantify complex samples of DNA containing both single-stranded DNA (ssDNA) and double-stranded DNA (dsDNA). Our protocol provides simple alterations of commercially available reagents and dyes for more reliable fluorometric quantification of DNA probes that contain both primary and secondary structures. Selective quantification of hybridized duplexes produced by DNA probes and complementary sequences also proves to be challenging due to the presence of unknown ratios of ssDNA and dsDNA. Another protocol is presented here for the quantification of dsDNA produced through hybridization events between DNA probes and complementary sequences. Enzymes for the selective digestion of unhybridized ssDNA are applied in this procedure to reduce background interference for better quantification of DNA hybridization. The advantages of this technique are presented in the following list:

- It is consistent for quantifying ssDNA and dsDNA probes of different sequence lengths.

- It employs well-established methods of DNA denaturation and sample cleanup.
- It uses simple instrumentation that is both cost-effective and sensitive.

Introduction

DNA nanostructures have diverse functionality in the realm of biotechnology and display the potential for vast application in point-of-care (POC) devices (1). DNA can take a variety of forms and exists in diverse structures, as a result of both unimolecular and bimolecular interactions. DNA probes exhibiting forms of unimolecular and bimolecular structure, such as hairpins and dangling ends, have been applied in DNA detection and quantification technologies, due to the more selective or sensitive hybridization that these structures provide (2, 3). To achieve a better understanding of how DNA with diverse structures interacts, there is a need for reliable, robust methods and instrumentation that can accurately quantify the amount of DNA regardless of structure. Two of the most common forms of measuring DNA concentration in a laboratory setting are spectrophotometry and fluorometry (4, 5). Spectrophotometry can be used to quantify the concentration of DNA based on Beer-Lambert's law (6). When using spectrophotometry, the amount of light absorbed at 260 nm is proportional to the amount of DNA present, while the ratio of absorbances for 260/280 and 260/230 nm can be used to determine sample purity (7). Fluorometric methods require the application of dyes or fluorochromes, which fluoresce corresponding to concentrations of DNA (8). Spectrophotometry utilizes small sample sizes and has the added benefit of no additional reagents (9). However, spectrophotometry does not provide specificity for differentiating ssDNA and dsDNA. Comparatively, fluorometric techniques provide more sensitive and selective detection for DNA quantification (5). The ability to measure low concentrations of DNA can be of utmost importance especially when working with samples that contain low concentrations of biomass

(10). Fluorochromes are capable of achieving quantification of concentrations lower than that of spectrometric means, as well as selective binding to ssDNA or dsDNA (11). Another available method is quantitative polymerase chain reaction (qPCR), which involves the combination of the amplification of target DNA alongside fluorometric techniques for quantification of specific DNA sequences. qPCR can involve the incorporation of dyes or functionalized DNA probes. Although a sensitive method for DNA quantification, the methodology requires application of specific primers, can be influenced by sample conditions, and does not differentiate between ssDNA and dsDNA (7).

Two instruments commonly found in laboratories that conduct spectrophotometric and fluorometric measurements for DNA quantification are the NanoDrop™ Spectrophotometer and Qubit™ Fluorometer (4). Comparative studies have claimed the Qubit to be more sensitive than the NanoDrop for quantifying DNA (12, 13). The Qubit also has specific dye that can differentiate dsDNA from ssDNA. Although the dsDNA Qubit assay is selective for dsDNA, one study has shown that the assay has the potential to measure up to 10% of ssDNA in solution (14). The ability to differentiate DNA structure can be crucial with samples that contain mixed concentrations of ssDNA and dsDNA or DNA structures that contain sequences of ssDNA and dsDNA. Variations of spectrophotometric and fluorometric techniques have been applied to detect DNA interactions, such as denaturation and hybridization. For example, shifts in absorbance can be utilized to determine changes in DNA through the NanoDrop. Such methods have been used to evaluate effectiveness of different types of denaturation methods (15, 16) or the presence of different DNA structures (17). However, since the spectrophotometric method is not strictly specific to each structure, spectrophotometry might not be the most reliable method for quantification of hybridization. Fluorometry has been effectively utilized to quantify

hybridization via labeling DNA probes with fluorophores or quenchers that either fluoresce or stop fluorescing after hybridizing with the complimentary strand. The change in fluorescence can be used to quantify the hybridization event (18). Unfortunately, synthesizing such DNA is expensive (19, 20). In a sample containing unknown ratios of hybridized duplexes, DNA probes, and complementary sequences, it is currently not possible to discern how much of the signal is generated by ssDNA or dsDNA, without additional sample treatment or functionalization.

In this chapter, two methods are presented through utilization of the Qubit fluorometer and compatible assays: one method for the quantification of DNA probes that contain secondary structure and another method for the quantification of dsDNA post-hybridization. Through this study, an effective form of DNA denaturation that is compatible with the Qubit ssDNA quantification assay is identified. In addition, enzymatic treatment is proposed as a method of sample cleanup and signal amplification of dsDNA resulting from hybridization.

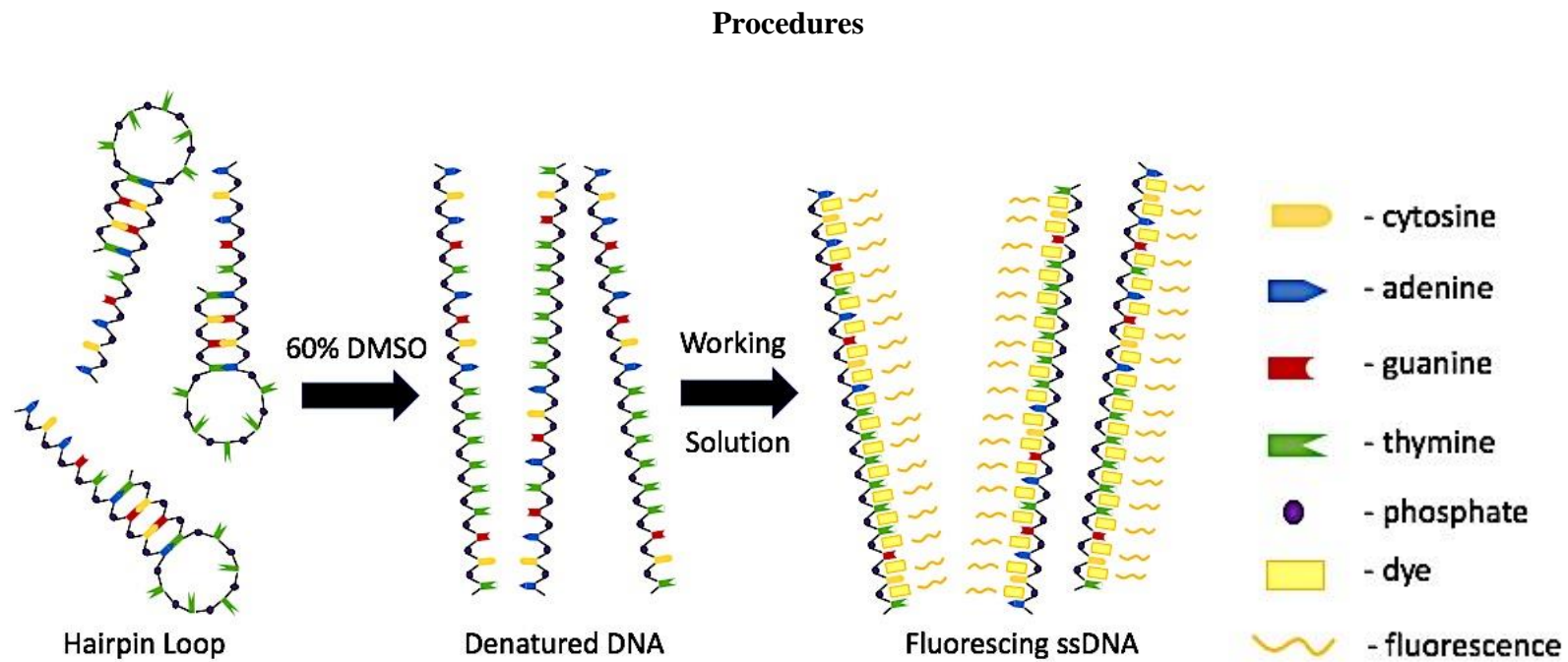


Figure 2.1. Schematic of the process for quantification of structured DNA probes via denaturation with DMSO followed by fluorescent dye treatment.

Quantification of Structured DNA Probes

1. Stock solutions of ssDNA that spanned the desired concentration range were created. In this study, the linear calibration was in the range of 2.24 – 16.5 ng/ μ L. Two stocks were made, since two different sources of ssDNA were used.
2. The Qubit fluorometer was calibrated using standards provided in the quantification kit.
3. The ssDNA quantification kit was used as described by the manufacturer to obtain measurements for dilutions spanning 2.24 – 16.5 ng/ μ L of ssDNA. A total volume of each dilution to be at least 36 μ L was made to have enough sample for measurements with and without DMSO. Each source of ssDNA was prepared at 3 different concentrations to yield a triplicate data set.
 - a. The dilutions were conducted by adding different ratios of ssDNA from the stock solution to ultrapure water. Ultimately, the sample was diluted again by adding 4 μ L of the sample to 6 μ L of ultrapure water.
 - b. After these two dilutions, 9 μ L of the sample was used for quantification. This specific dilution sequence was important for the later application of DMSO.
4. The new assay mix with DMSO was created, and the total volume of assay was determined by multiplying the number of measurements by 200 μ L; of the total volume, 60% was DMSO and the remaining 40% was the buffer and dye provided in the assay kit. For example, for 18 samples, the total volume was 3600 μ L, with 2160 μ L of that being DMSO, 1422 μ L of buffer, and 18 μ L of dye.
5. The assay mixture was vortexed, and the container holding the assay mixture was ensured to not be composed of a material that reacted with DMSO.
6. The same dilutions of ssDNA from the first set of measurements were used.

7. Next step consisted of another dilution, yet this time, using 6 μL of DMSO and 4 μL of the diluted sample, instead of ultrapure water.
8. The DNA sample was allowed to incubate in the DMSO for 1 minute at room temperature.
9. Finally, 191 μL of the assay mix and 9 μL of the DNA mixed with DMSO were pipetted into a 500 μL PCR tube for measurement in the Qubit fluorometer.
10. The mixture was vortexed for approximately 3 seconds and incubated for 2 minutes at room temperature.
11. Since the concentrations of ssDNA were identical for both applied assays, the concentrations reported for the traditional application of the quantification assay were matched to the raw relative fluorescence units (RFUs) generated by the samples mixed with DMSO to create a linear calibration curve.
12. With the calibration curve constructed, DNA of diverse secondary structures can be treated with DMSO and the altered assay mix applied to quantify the amount of ssDNA present.

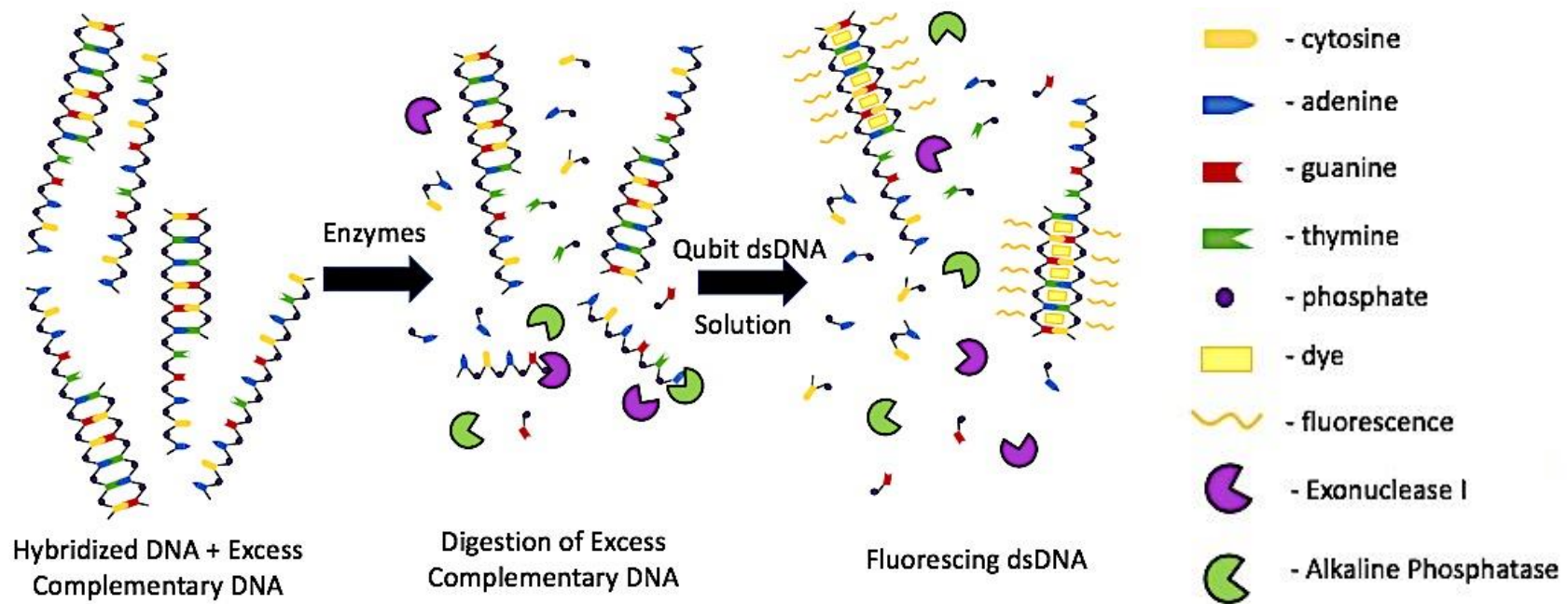


Figure 2.2. Schematic of the process for quantification of DNA hybridization via enzymatic digestion followed by fluorescent dye treatment.

Quantification of DNA Hybridization

1. The maximum concentration of complementary ssDNA that would be in the samples if no DNA hybridization occurred was calculated. For our specific application, it was calculated that if no target strand hybridized, 22.1 ng/ μ L of the target strand would be present in solution during measurement. Next, the maximum concentration of dsDNA that would be in the samples if complete hybridization occurred was calculated. Since only 8.25×10^{10} copies/ μ L of probe would be present during the measurement that was also the maximum concentration of hybridized duplexes possible. For this calibration, the source of dsDNA was a 167-mer amplified via PCR.
2. With the maximum concentrations of DNA determined, stock solutions of ssDNA and dsDNA were created that covered the desired concentration ranges.
3. The Qubit fluorometer was calibrated using standards provided in the dsDNA quantification kit.
4. The dsDNA quantification kit was used as described by the supplier and measurements for dilutions of dsDNA across predicted concentration range was obtained.
5. Similarly, dilutions with dsDNA across the predicted range of hybridized DNA was created, as done in the previous step, except it was spiked with ssDNA. For this study, to determine the influence of the ssDNA on the method, the range of dsDNA was tested in the presence of both 11.0 ng/ μ L and 22.1 ng/ μ L of ssDNA. Also, one set was tested without any ssDNA to determine the influence of the enzyme on dsDNA.
6. Next, the samples containing mixed ratios of ssDNA and dsDNA were enzymatically treated. Five μ L of the sample was transferred to a new 200 μ L PCR tube. To this tube, 2 μ L of FastAP buffer, 1 μ L of FastAP Alkaline Phosphatase, 1 μ L of Exonuclease buffer, and 1 μ L of Exonuclease I were also added.

7. The tube was then placed in the thermocycler to incubate for 2 hours at 37°C.
8. Then, the dsDNA was quantified using the Qubit fluorometer as described by the manufacturer. For our data acquisition, 9 μ L of the sample was used.
9. Since the concentrations of dsDNA were identically prepared for both applied assays, the concentrations reported for dsDNA in the absence of ssDNA were matched to the raw RFUs generated by the samples spiked with different concentrations of ssDNA to generate a linear calibration.
10. By using the obtained calibration curve, the dsDNA formed by hybridization can be better quantified without excessive noise being generated by strands of unhybridized ssDNA.

Additional Information and Method Validation

Isolation of DNA structure was a pivotal step to accurately quantify DNA with different structures via this developed methodology. Both sodium hydroxide (NaOH) and dimethyl sulfoxide (DMSO) were explored as options for chemical denaturation. For the described method, all DNA probes were dissolved in ultrapure water; thus, the sample pH was simple to regulate, and NaOH was initially examined as a chemical denaturant. Furthermore, the mechanism of denaturation induced by a basic pH is a well-documented process of disrupting secondary structure through hydrolysis of the hydrogen bonds that construct the backbone of DNA (21, 22). The NanoDrop was first considered to measure the DNA concentration, as it is commonly used for DNA quantification, does not require the use of additional chemicals or buffers, and considering that the samples sizes were small. Before measurement with the NanoDrop, samples were diluted in half with a solution of NaOH. To have a comparative reference, samples with the same DNA concentrations were prepared for quantification via the

Qubit. As a means to examine the quantification consistency between the NanoDrop and Qubit, two sources of ssDNA were tested; one was a 30-mer and the other a 52-mer, both of which were diluted and measured at five different concentrations respective to the source on both instruments, as seen in Fig. 2.3.

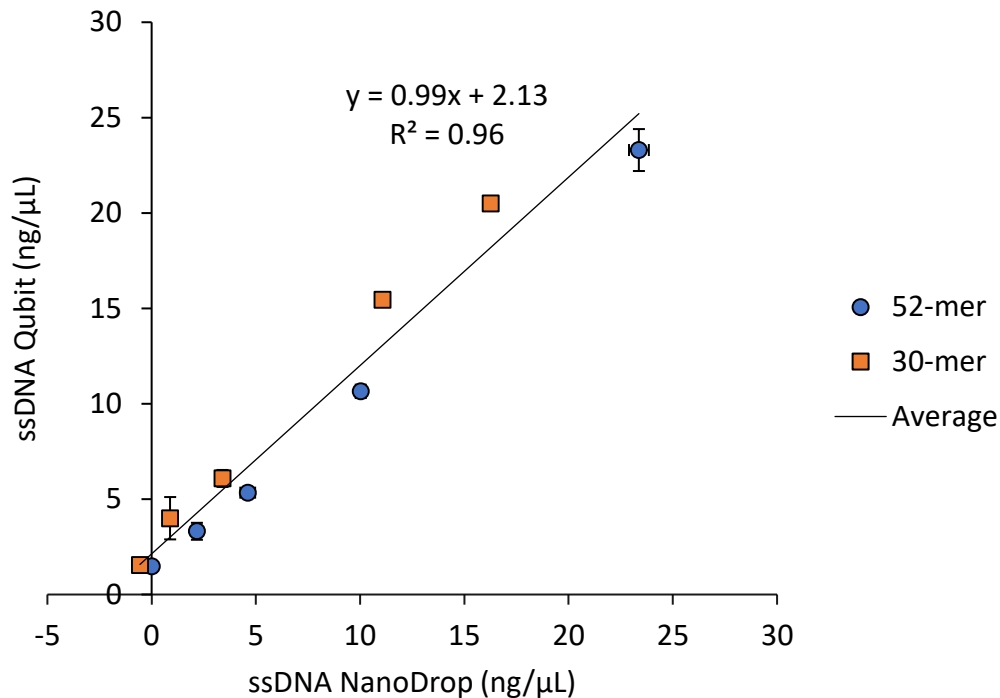


Figure 2.3. Comparison between ssDNA concentrations measured with Qubit and NanoDrop. Samples for each form of measurement with respective instrument were done in duplicate. Error bars are provided for both axes and represent standard deviations.

Although the linear regression for the averaged data (shown in Fig. 2.3) yields a relationship that is nearly one-to-one, the y-intercept does not cross at zero. As displayed by the y-intercept, in the lower concentrations tested, the Qubit was still quantifying DNA, opposed to the NanoDrop, which was reporting negative values. In one study, the NanoDrop was not capable of producing reliable measurements below concentrations of 30 ng/μL (23). In comparative studies with the Qubit, the NanoDrop is often cited as overestimating DNA

concentrations (4, 24, 25), unlike the data presented in Fig. 2.3. Yet, those studies focused on quantification of dsDNA. In a different study, the ssDNA Qubit assay consistently reported higher concentrations of ssDNA, compared to the NanoDrop; the Qubit was claimed to have higher sensitivity, aiding in the ability to quantify low concentrations of DNA (12). However, it should be noted that the ssDNA Qubit assay is not strictly specific to ssDNA, meaning the signal could have been supplemented by dsDNA sequences. As seen by the R^2 of 0.96 (Fig. 2.3), for this tested concentration range, the length of DNA sequence did not have a major impact on the quantification. Regardless, the inability to quantify DNA concentrations below 4 ng/ μ L, dictated the choice to consider the more sensitive Qubit instrument, even with the necessary sample preparation. Although the buffers and dyes provided in the Qubit quantification kits are proprietary, Thermo Fisher Scientific does promote the versatility of the device and has a webtool to aid in the creation of custom Qubit assays that can be uploaded to the Qubit fluorometer (26). Since NaOH was considered as a denaturation method for the DNA samples, in conjunction with the Qubit assay, it was necessary to increase the pH of the buffered proprietary working solution created for the measurement. Unfortunately, the success of the fluorescent signal appeared to be pH dependent and increasing the pH prevented the dye from either effectively binding or fluorescing. To circumvent this problem, DMSO was considered as a chemical agent for denaturation. Furthermore, in a recent study comparing methods for DNA denaturation, a solution of 60% DMSO was the most effective chemical means of denaturation reviewed (15). DMSO destabilizes the base stacking interactions that lead to the ultimate disruption in secondary structure, and thus, ssDNA (17). Although sensitivity of the assay was reduced when a considerable amount of the working solution was replaced with DMSO, a viable range was obtained, which yielded the formation of a linear calibration, as seen in Fig. 2.4. The

data collected for Fig. 2.4 was completed by following the steps presented earlier for quantification of structured DNA probes.

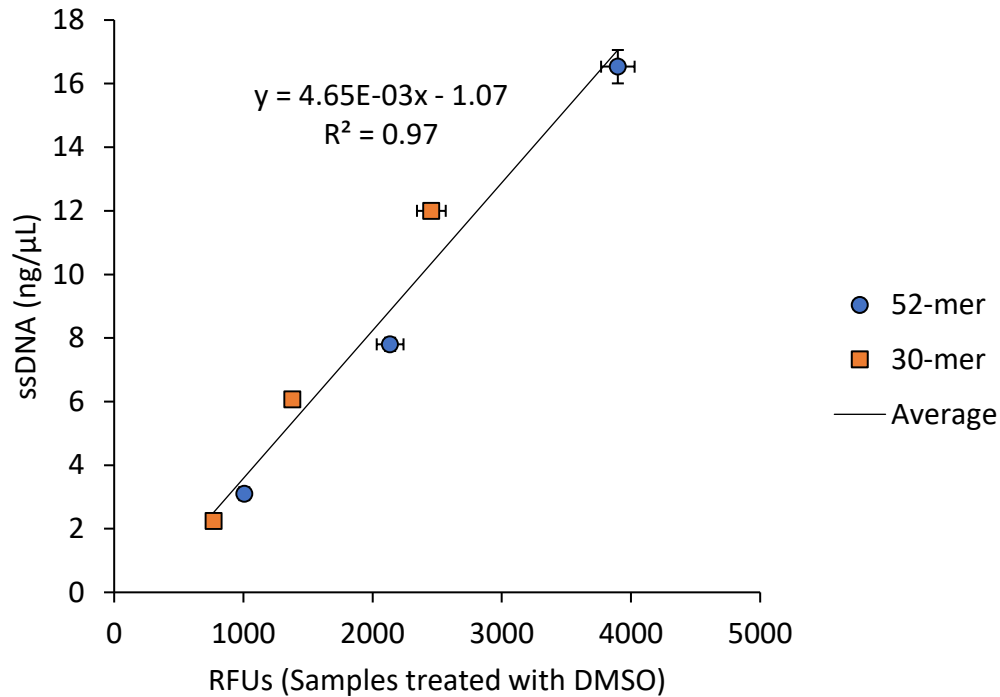


Figure 2.4. Linear calibration for the determination of ssDNA concentration dissolved in DMSO. Samples for each data point were made in triplicate, created under identical sample preparation, and the error bars represent standard deviations.

The dye provided in the quantification kit is stored in DMSO, which could be a contributing factor as to how the assay still produced a quantifiable and discernable signal when mixed with a high ratio of DMSO. Once again, for this tested concentration range, the R^2 value of 0.97 indicates a strong linear relationship, regardless of applied sequence length.

Similar to the issues confronted with quantification of structured DNA probes, quantifying hybridization is also challenging based on differentiating ssDNA and dsDNA. However, this issue cannot be solved by denaturation. DNA hybridization occurs between two complementary strands, but based on the conditions in the sample, not all DNA probes will

hybridize into a duplex (27). Furthermore, to ensure maximum hybridization of the DNA probe, DNA is traditionally provided in excess, potentially leaving a high concentration of unhybridized ssDNA in solution (28). To demonstrate the effect of background interference from ssDNA, samples were prepared with the same concentrations of dsDNA, and then spiked with concentrations of ssDNA. As the concentration of ssDNA increased in solution, sensitivity of the dsDNA Qubit assay to dsDNA was reduced, as seen in Fig. 2.5.

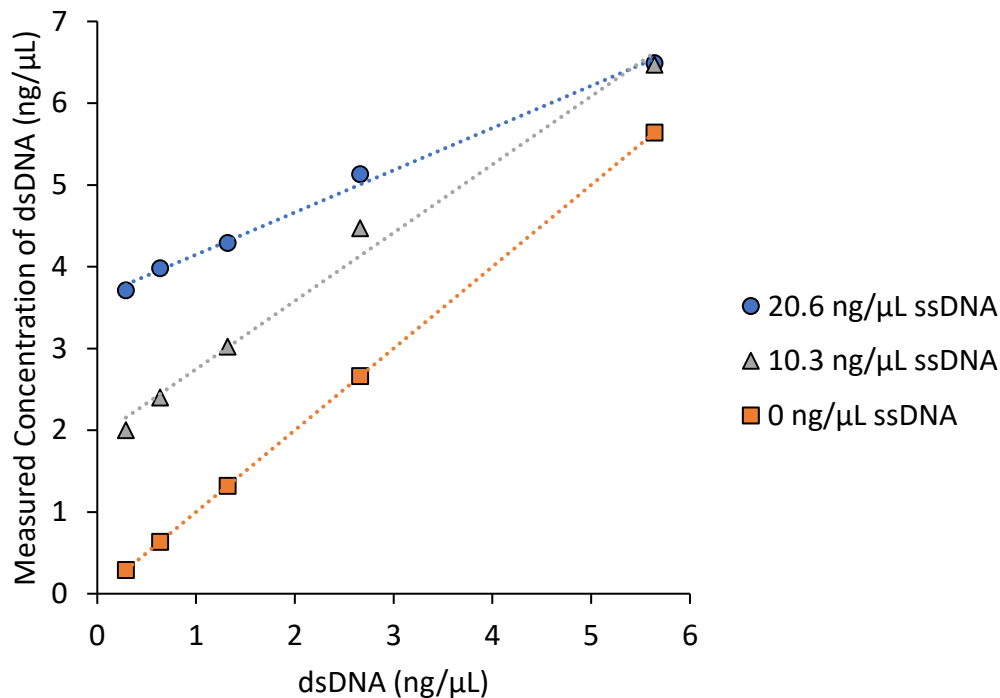


Figure 2.5. Measured concentrations of dsDNA spiked with concentrations of ssDNA to assess the effect of ssDNA on background noise. Each linear relationship represents solutions produced with the same concentration of dsDNA but in the presence of different concentrations of ssDNA.

Therefore, the primary objective was to isolate the hybridized duplex through elimination of the unhybridized ssDNA. Removal of the excess unhybridized ssDNA would induce a reduction in background noise and allow for more accurate quantification of hybridization.

Various types of enzymes exist for the specific digestion of particular DNA structures.

Exonucleases are a family of enzymes that have the potential to digest any form of DNA (29). Exonuclease I is an enzyme that specifically digests ssDNA by binding to the 3' end of the DNA and releasing deoxyribocucleoside 5' monophosphate, ultimately leaving the 5' termini dinucleotide intact. This type of exonuclease has application for purification of samples to remove excess primers after PCR (30). Even though noise reduction was possible via application of the enzymes, it was important to calibrate at the concentrations of ssDNA that the enzymes must digest, to accurately determine the amount of dsDNA in solution. Using the calibration generated in Fig. 2.6, the samples treated in the predetermined range of ratios of ssDNA and dsDNA could be quantified. The data collected for Fig. 2.6 was achieved by following the steps presented earlier for quantification of dsDNA from hybridization. Samples created and measured for Figs. 2.5 and 2.6 were created in the same manner; however, those presented in Fig. 2.6 were exposed to exonuclease I. By comparing Figs. 2.5 and 2.6, the clear decrease in background noise proves the enzymatic cleanup to be an effective method for reduction of unwanted signal production from unhybridized ssDNA. Based on knowledge of potential concentration ranges for dsDNA and ssDNA, similar calibration curves can be created for other hybridization experiments. Although the difference in sequence length did not appear to affect the linearity of data presented in Figs. 2.4 and 2.5, fragmentation of DNA has been noted to influence fluorescence production used for DNA quantification. Therefore, when applying this method for the quantification of hybridization events, it is advisable to use ssDNA and dsDNA lengths comparable to those being studied (7). Furthermore, a possible limitation of this methodology could be the quantifiable range. Hybridization is commonly fabricated in DNA assays by creating a ratio of the complementary sequences that surpasses unity (31, 32).

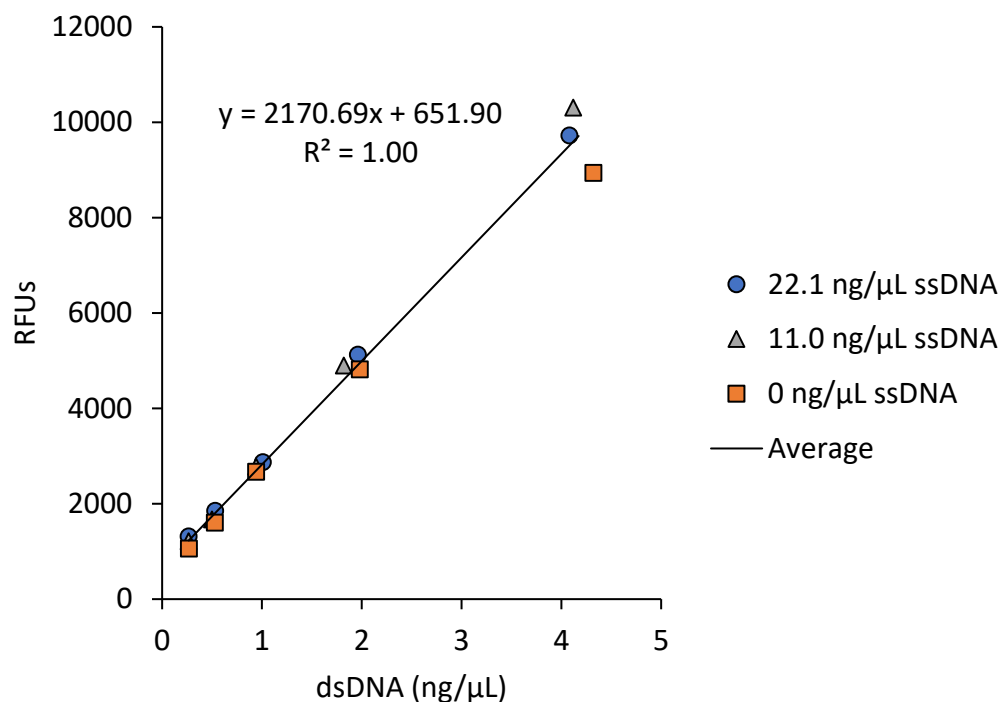


Figure 2.6. Concentrations of dsDNA spiked with concentrations of ssDNA and treated with Exonuclease I. Each color represents solutions produced with the same concentration of dsDNA, but in the presence of different concentrations of ssDNA followed by enzymatic cleanup.

Based on known concentrations for an experiment, the enzymes should be tested to ensure that the background noise can be successfully dampened, especially if the ssDNA concentrations surpass those in Fig. 2.6. For the purposes of this study, calibration for dsDNA was generated with the maximum and half the maximum concentration of target strand applied to the samples.

Conclusions

The Qubit ssDNA assay and dsDNA high sensitivity assay kits were utilized to provide more accurate quantification of structured DNA probes and hybridized duplexes. The ssDNA assay was used in conjunction with DMSO to denature any unimolecular folding and ensure the measurement of only ssDNA. This protocol allows for probes that contain secondary structure, such as hairpins, to be accurately quantified. Samples used with the dsDNA assay for quantification of hybridization were pretreated with exonuclease I for the specific digestion of

unhybridized ssDNA. This additional treatment step allows for the quantification of hybridized DNA without the need to synthesize DNA with fluorescent tags. Both of these methods utilize instrumentation and chemicals that are affordable and widely used for DNA analysis and are overall achieved by following simple steps. Furthermore, the application of fluorometric techniques provides more sensitive measurements at lower concentrations, compared to other methods that employ spectrophotometric techniques.

References

1. Mathur,D. and Medintz,I.L. (2019) The Growing Development of DNA Nanostructures for Potential Healthcare-Related Applications. *Adv. Healthc. Mater.*, **8**.
2. Miranda-Castro,R., De-los-Santos-Álvarez,N., Lobo-Castañón,M.J., Miranda-Ordieres,A.J. and Tuñón-Blanco,P. (2009) Structured nucleic acid probes for electrochemical devices. *Electroanalysis*, **21**, 2077–2090.
3. Broude,N.E. (2002) Stem-loop oligonucleotides: A robust tool for molecular biology and biotechnology. *Trends Biotechnol.*, **20**, 249–256.
4. Simbolo,M., Gottardi,M., Corbo,V., Fassan,M., Mafficini,A., Malpeli,G., Lawlor,R.T. and Scarpa,A. (2013) DNA Qualification Workflow for Next Generation Sequencing of Histopathological Samples. *PLoS One*, **8**.
5. Sedlackova,T., Repiska,G., Celec,P., Szemes,T. and Minarik,G. (2013) Fragmentation of DNA affects the accuracy of the DNA quantitation by the commonly used methods. *Biol. Proced. Online*, **15**, 1–8.
6. Leclerc,O., Fraisse,P.O., Labarraque,G., Oster,C., Pichaut,J.P., Baume,M., Jarraud,S., Fisticaro,P. and Vaslin-Reimann,S. (2013) Method development for genomic *Legionella pneumophila* DNA quantification by inductively coupled plasma mass spectrometry. *Anal. Biochem.*, **435**, 153–158.
7. Gryson,N. (2010) Effect of food processing on plant DNA degradation and PCR-based GMO analysis: A review. *Anal. Bioanal. Chem.*, **396**, 2003–2022.
8. Kumar,D., Panigrahi,M.K., Suryavanshi,M., Mehta,A. and Saikia,K.K. (2016) Quantification of DNA extracted from formalin fixed paraffin-embedded tissue comparison of three techniques: Effect on PCR efficiency. *J. Clin. Diagnostic Res.*, **10**, 3–5.
9. Desjardins,P. and Conklin,D. (2010) NanoDrop microvolume quantitation of nucleic acids. *J. Vis. Exp.*, 10.3791/2565.

10. Wang,H., Bédard,E., Prévost,M., Camper,A.K., Hill,V.R. and Pruden,A. (2017) Methodological approaches for monitoring opportunistic pathogens in premise plumbing: A review. *Water Res.*, **117**, 68–86.
11. Nielsen,K., Mogensen,H.S., Hedman,J., Niederstätter,H., Parson,W. and Morling,N. (2008) Comparison of five DNA quantification methods. *Forensic Sci. Int. Genet.*, **2**, 226–230.
12. Ponti,G., Maccaferri,M., Manfredini,M., Kaleci,S., Mandrioli,M., Pellacani,G., Ozben,T., Depenni,R., Bianchi,G., Pirola,G.M., *et al.* (2018) The value of fluorimetry (Qubit) and spectrophotometry (NanoDrop) in the quantification of cell-free DNA (cfDNA) in malignant melanoma and prostate cancer patients. *Clin. Chim. Acta*, **479**, 14–19.
13. Sarnecka,A.K., Nawrat,D., Piwowar,M., Ligęza,J., Swadźba,J. and Wójcik,P. (2019) DNA extraction from FFPE tissue samples – a comparison of three procedures. *Wspolczesna Onkol.*, **23**, 52–58.
14. Invitrogen (2016) Qubit dsDNA assay specificity in the presence of single-stranded DNA.
15. Wang,X., Jeong Lim,H. and Son,A. (2014) Characterization of denaturation and renaturation of DNA for DNA hybridization. *Environ. Health Toxicol.*, **29**, 8.
16. Hirschman,S.Z. and Felsenfeld,G. (1966) Determination of DNA composition and concentration by spectral analysis. *J. Mol. Biol.*, **16**, 347–358.
17. Nwokeoji,A.O., Kilby,P.M., Portwood,D.E. and Dickman,M.J. (2017) Accurate Quantification of Nucleic Acids Using Hypochromicity Measurements in Conjunction with UV Spectrophotometry. *Anal. Chem.*, **89**, 13567–13574.
18. Moreira,B.G., You,Y., Behlke,M.A. and Owczarzy,R. (2005) Effects of fluorescent dyes, quenchers, and dangling ends on DNA duplex stability. *Biochem. Biophys. Res. Commun.*, **327**, 473–484.
19. Zhang,J.X., Fang,J.Z., Duan,W., Wu,L.R., Zhang,A.W., Dalchau,N., Yordanov,B., Petersen,R., Phillips,A. and Zhang,D.Y. (2018) Predicting DNA hybridization kinetics from sequence. *Nat. Chem.*, **10**, 91–98.
20. Kolpashchikov,D.M. (2019) Evolution of Hybridization Probes to DNA Machines and Robots. *Acc. Chem. Res.*, **52**, 1949–1956.
21. Ageno,M., Dore,E. and Frontali,C. (1969) The Alkaline Denaturation of DNA. *Biophys. J.*, **9**, 1281–1311.
22. Shooter,K. V. (1976) The kinetics of the alkaline hydrolysis of phosphotriesters in DNA. *Chem. Biol. Interact.*, **13**, 151–163.
23. Yu,S., Wang,Y., Li,X., Yu,F. and Li,W. (2017) The factors affecting the reproducibility of micro-volume DNA mass quantification in Nanodrop 2000 spectrophotometer. *Optik (Stuttg.)*, **145**, 555–560.

24. Nakayama, Y., Yamaguchi, H., Einaga, N. and Esumi, M. (2016) Pitfalls of DNA quantification using DNA-binding fluorescent dyes and suggested solutions. *PLoS One*, **11**, 1–12.
25. O’Neill, M., McPartlin, J., Arthur, K., Riedel, S. and McMillan, N.D. (2011) Comparison of the TLDA with the nanodrop and the reference qubit system. *J. Phys. Conf. Ser.*, **307**.
26. Thermo Fisher Scientific. (2018) Qubit™ 4 Fluorometer User Guide Qubit.
27. Wetmur, J.G. and Fresco, J. (1991) DNA probes: Applications of the principles of nucleic acid hybridization. *Crit. Rev. Biochem. Mol. Biol.*, **26**, 227–259.
28. Narayanan, S. (1992) Overview of principles and current uses of DNA probes in clinical and laboratory medicine. *Ann. Clin. Lab. Sci.*, **22**, 353–376.
29. Thomas, K.R. and Olivera, B.M. (1978) Processivity of DNA exonucleases. *J. Biol. Chem.*, **253**, 424–429.
30. Thermo Fisher Scientific (2012) Product info: Exonuclease I.
31. Steger, D., Berry, D., Haider, S., Horn, M., Wagner, M., Stocker, R. and Loy, A. (2011) Systematic spatial bias in DNA microarray hybridization is caused by probe spot position-dependent variability in lateral diffusion. *PLoS One*, **6**, 1–11.
32. Deng, J., Shoemaker, R., Xie, B., Gore, A., Leproust, E.M., Antosiewicz-Bourget, J., Egli, D., Maherali, N., Park, I.H., Yu, J., *et al.* (2009) Targeted bisulfite sequencing reveals changes in DNA methylation associated with nuclear reprogramming. *Nat. Biotechnol.*, **27**, 353–360.

CHAPTER 3. THE EFFECT OF STRUCTURE ON DNA HYBRIDIZATION IN SOLUTION AND IMMOBILIZED ON A PARTICLE SURFACE FOR OPTIMIZED DETECTION OF *LEGIONELLA PNEUMOPHILA*

Parker Dulin¹, Carmen Gomes², Kaoru Ikuma¹

¹Department of Civil, Construction and Environmental Engineering, Iowa State University, USA

²Department of Mechanical Engineering, Iowa State University, USA

Modified from a manuscript to be submitted to *Nucleic Acids Research*

Abstract

Reported cases of Legionnaires' disease have increased significantly in recent years. The need for sensitive methods with faster turnaround time than culture methods for detecting *L. pneumophila* is rising. DNA-based biosensors can serve as applicable tools for *in situ* pathogen monitoring and detection. In this research, we investigated the application of DNA probes targeting *L. pneumophila* with a dangling-ended hairpin structure compared to more traditional linear structures to determine if the presence of the secondary structure improved hybridization, and ultimately *L. pneumophila* detection. Hybridization of the probes to the target DNA sequence was measured at different DNA concentrations while unbound and immobilized on a magnetic microparticle surface. When unbound, the linear signal probe (LSP), observed higher sensitivity compared to the dangling-ended hairpin probe (Key) for hybridization with the target DNA sequence. The LSP and Key exhibited slopes of 1.88 and 1.06; respectively, for the range of concentrations tested. When immobilized on a particle surface, the difference displayed in hybridization between the probes was not significant. However, when compared to the unbound probes, the immobilized probes observed overall higher percentages of hybridization. The increased hybridization exhibited by the immobilized probes, when compared to the unbound probes, displays the importance of ionic strength for DNA hybridization, regardless of

immobilization or DNA structure. Therefore, unbound linear DNA probes utilized for detection in solutions absent of ionic strength provided more sensitive detection than dangling-ended probes. However after immobilization, probe structure did not yield a significant change in sensitivity for detection, in the applied sample conditions. Ultimately, immobilizing DNA and hybridizing in ionic conditions, regardless of structure, could lead to more sensitive and functional biosensors, when compared to conducting hybridization in solutions at low ionic strength.

Introduction

To protect public health and ensure water quality, known pathogenic threats need to be monitored. Monitoring for dangerous pathogens allows for rapid response to contamination, preventing the spread of disease while protecting the public (1). However, conventional culture methods of pathogenic monitoring are constrained by representative sampling and lengthy response times (2). Biosensors have gained attention as a potential solution to *in situ* monitoring for pollutants in water (3, 4). DNA-based biosensors in particular are selective, simple, cost-effective, and fast (5). Unlike other bioreceptors, DNA can be chemically synthesized (6), and hybridization events create the potential for reagentless detection and can be regenerated for reuse, meaning the device will not be limited to one-time usage (7, 8). In addition, nucleic acids have been noted as a powerful tool for parallel detection of multiple pathogenic threats and have been applied to form microarray-based detection schemes (5).

L. pneumophila remains a public health issue and is presently one of the most threatening waterborne pathogens, particularly in developed countries (9). According to the Centers for Disease Control (CDC) and the National Notifiable Diseases Surveillance System (NNDSS), reported cases of Legionnaires' disease have increased over five times since the turn of the century. Although it is unclear whether the source of the dramatic increase indicates an

increasing immunologically susceptible population, increasing awareness of testing and diagnosis, or increasing prevalence of *Legionella* (10), it is clear that this is a serious public health concern that could be better mitigated by improved forms of detection of the pathogen before human exposure. The commonly practiced method of monitoring for pathogens via culturing has been noted as unreliable since *Legionella* cells can exist in a viable but non-culturable state (VBNC) as well as inside amoeba (11). However, molecular methods have faster response times and are capable of detecting VBNC cells, while maintaining sensitivity and selectivity (2). A variety of DNA-based detection and quantification schemes for *Legionella* has been reported (12–14). The DNA structures and materials for these biosensing devices are diverse and the options for design are almost limitless. Detection and quantification are important to contain an outbreak, and more sensitive devices will further protect those individuals with compromised immune systems that are most at risk. Thus, there is a strong need for more development and optimization of technologies and techniques focused on the detection and quantification of pathogens to protect water quality and public health (2).

At the crux of a DNA-based biosensor is DNA hybridization. Understanding hybridization is pivotal to the success of implementing DNA as a bioreceptor. Factors influencing hybridization and the stability of DNA duplexes include temperature, solution composition, sequence composition, and structure (15). As the field of DNA-based biosensors has grown, there has been diverse application of DNA in different structural forms. Understanding how structural differences of the DNA influence binding affinity is beneficial to the application of nucleic acids in biosensors. The impact of secondary structure on hybridization has been noted in previous studies (16–19). Hairpin DNA structures have seen wide application in biosensors due to their functionality for signal production and control during hybridization; in

fact, various studies have highlighted the ability for secondary structure to improve hybridization, and thus, the selectivity or sensitivity of the biosensor (20, 21). In the context of a biosensor, hybridization commonly involves immobilized DNA probes. Hybridization with surface-tethered DNA introduces other factors, such as probe density and surface geometry (22). Considering all the potential factors, more studies are necessary to develop an improved understanding of how DNA structure influences hybridization, whether in solution or immobilized.

This research focuses on designing a sensitive probe for DNA hybridization, by comparing the feasibility of linear DNA and hairpin DNA with a dangling end as signal probes for application in a biosensor for the detection of *L. pneumophila*. Furthermore, a comparison is presented of hybridization both in solution and immobilized on a magnetic particle, for a more holistic picture of how immobilization and DNA structure influences hybridization. Understanding these influences will contribute to designing biosensors with improved performance, which includes high selectivity toward target pathogen, lower limits of detection, and detection ranges to quantify relevant pathogens to protect public health.

Materials and Methods

All oligonucleotide sequences were synthesized by IDT (Integrated DNA Technologies, Coraville, IA). The name, function, sequence, and modification of each DNA probe are provided in Table 3.1. Application of DNA with the same sequences has been reported for research conducted on biosensing methods for detection of *L. pneumophila* (12, 17), as well as the use of the hairpin structure (21, 23). The scrambled sequences were randomly generated in MATLAB and searched using the National Center for Biotechnology Information Basic Local Alignment Search Tool (BLAST) database to ensure the absence of unwanted hybridization. The probes without biotin were utilized in the solution study and were purified via desalting. The linear

signal probe with biotin was also purified via desalting. However, since the hairpin signal probe with biotin involved internal modification, desalting was not available as a purification method. Therefore, the hairpin with biotin was purified through high performance liquid chromatography (HPLC). Throughout this study, the DNA probes are referenced by the names provided in Table 3.1.

Table 3.1. List of the DNA sequences employed for all aspects of this study.

Name	Function	Oligonucleotide Sequence 5' → 3'	References
TS	Target	AAGTTATCTGTGAATTCCTGGGCTTAACCTGGGACGACGGTCAGATAATACTGG	(14, 17)
LSP	Linear Signal Probe	GGTTAAGCCCAGGAATTTACAGATAACTT	(14, 17)
Key	Hairpin Signal Probe	GGTTAAGCCCAGGAATTTACAGATAACTTGATCAGCTGCACGTTUTTCCTGGTGCAGC TGAT	(14, 17, 21)*
Bio-LSP	Linear Signal Probe with Biotin	GGTTAAGCCCAGAATTCACAGATAACTT /iSp18//iSp18//iSpC3//3Bio/	(14, 17)*
Bio-Key	Hairpin Signal Probe with Biotin	GGTTAAGCCCAGGAATTTACAGATAACTTGATCAGCTGCACCAGGTT /iBiodT/TTCCTGGTGCAGCTGATC	(14, 17, 21)*
Scrambled LSP	Selectivity Control	CGGTAATAAGTGCTCCATAGTTCATGAAAC	N/A
Scrambled Key	Selectivity Control	CGGTAATAAGTGCTCCATAGTTCATGAAACGATCAGCTGCACCAGGTTUTTCCTGGTGC AGCTGATC	N/A
*iSp18 - Carbon chain spacer of 18 carbons			
*iSpC3 - Carbon chain spacer of 3 carbons			
*3Bio - Biotin located on the 3' end			
*iBiodT - Biotin conjugated with a thymine group			
*The Key structure combined a hairpin sequence from one study (21) and the dangling-end was the same sequence as the LSP (14)			
*Bio-LSP was the same DNA sequence as the LSP with biotin and carbon chain spacer			
*Bio-Key was the same DNA sequence as the Key with biotin in the center of the hairpin loop			

Solution Study

Ultrapure water (Invitrogen, Carlsbad, CA), target DNA, and the respective DNA probes were added to make each 15 μ L sample. With the eventual application of enzymes to the samples, ultrapure water was utilized for the reaction matrix to avoid problems with decreased enzymatic efficiency. The stock concentrations for each DNA source were determined using the Qubit single-stranded DNA (ssDNA) assay with dimethyl sulfoxide (DMSO). The secondary structure of the hairpin was disrupted by DMSO through destabilization of the base-stacking interactions to create linear DNA for accurate measurements (24) (see Chapter 2 for method development).

All DNA probes were quantified using a linear calibration curve shown in Fig. 3.1, generated in a working solution of 60% DMSO, with the remaining 40% as the buffer and dye provided in the Qubit ssDNA assay kit. The calibration curve was created by diluting a solution of ssDNA through the known range of quantification and measuring the Relative Fluorescence Units (RFUs) of the dilutions with the ssDNA assay kit, followed by measuring samples of the same dilutions in the altered working solution containing 60% DMSO. To ensure that the measurements were not skewed by sequence length, this linear calibration curve was prepared using two different sources of linear ssDNA. For the six data points displayed, three were produced from a ssDNA source of 30 bases and the other three were produced from a ssDNA source of 52 bases. All samples were produced in triplicate.

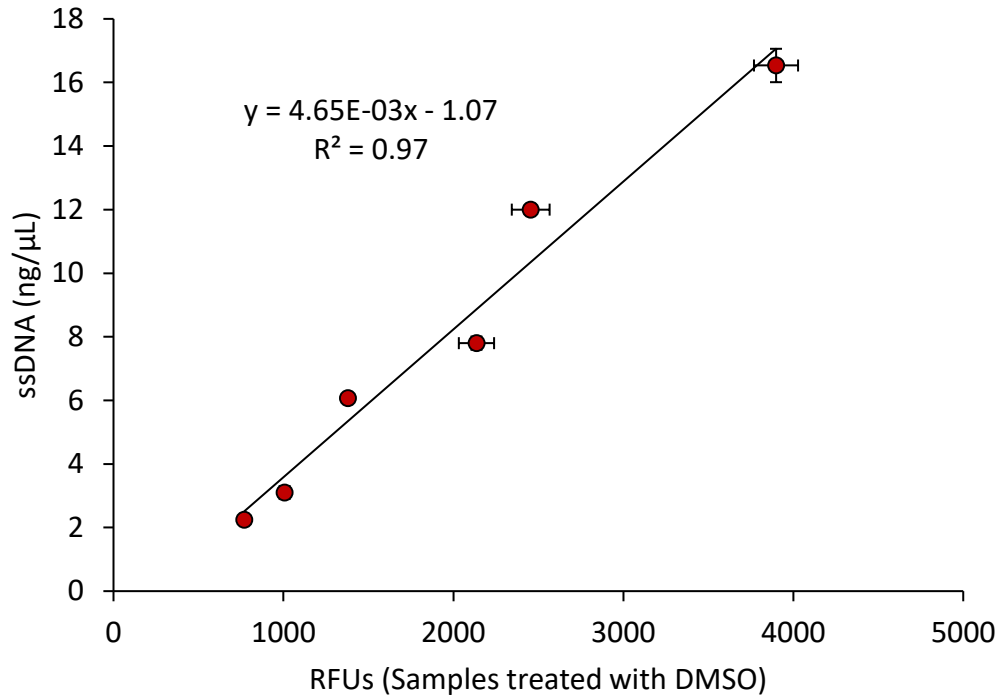


Figure 3.1. Linear calibration for the determination of ssDNA concentration dissolved in DMSO. Samples for each data point were made in triplicate, created under identical sample preparation, and the error bars represent standard deviations.

After quantification of the stock solutions, DNA was added at different concentrations to achieve desired ratios of target copies to probe copies, ranging from one to ten. The DNA mixtures were placed in a thermocycler at 90°C for 5 minutes, followed by an incubation period of 1 hour at room temperature for hybridization, similarly described by Zang et. al (25). After incubation, the samples were subjected to a cleanup step for the removal of unhybridized target sequences (see Chapter 2 for method development). Five μL from the hybridization reaction volume was removed and placed in a new PCR tube followed by addition of 1 μL of exonuclease I, 2 μL of thermosensitive alkaline phosphatase, and 1 μL of each enzyme's respective reaction buffer (ThermoFisher, Waltham, MA) to yield a total of 10 μL. The samples were incubated at 37°C for 2 hours for the enzymatic reaction to complete. At the conclusion of this second

incubation period, the amount of double-stranded DNA (dsDNA) present in the sample was quantified through the use of the Qubit dsDNA HS Assay Kit (ThermoFisher, Waltham, MA). To account for the complex composition of the sample containing dsDNA consisting of two different enzymes, and two different buffers, another calibration curve was generated for this situation, as shown in Fig. 3.2.

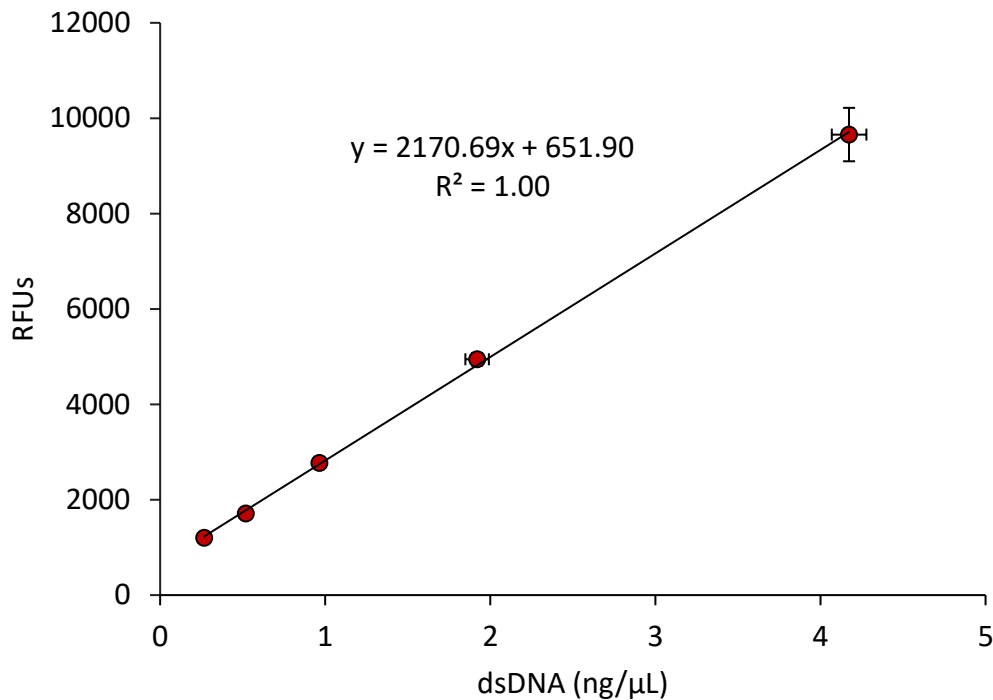


Figure 3.2. Linear calibration curve for quantification of dsDNA in the presence of ssDNA, enzymes used for cleanup, and respective buffers. Each data point represents averaged concentration of dsDNA for samples prepared in triplicate.

A known solution of dsDNA was diluted to provide calibration standards that covered dsDNA concentrations across a range that was expected to be observed post-hybridization. These solutions were individually measured in the presence of 0, 11.0, and 22.1 ng/μL of ssDNA after following the same cleanup procedure, yielding a triplicate data set. The solution of ssDNA used to spike the samples of dsDNA was quantified using the previous calibration presented in Fig.

3.1. Percent hybridization was defined as the measured number of hybridized copies divided by the number of potential hybridized copies multiplied by 100.

$$\% \text{ Hybridization} = \left(\frac{\text{Measured Copies}}{\text{Theoretical Copies}} \right) \times 100 \quad (1)$$

Particle Study

Quantification of functionalized DNA probes

Under the assumption that each DNA probe contained one biotin moiety, the Amplite Colorimetric Biotin Quantification Kit (AAT Bioquest, Sunnyvale, CA) was utilized to determine the biotin concentration and then was used to indirectly calculate the DNA probe concentrations. The assay was used according to the manufacturer's instructions in triplicate for both probes, with 10 μL for the sample size (26). With the concentrations of DNA known for each probe, stock volumes were created by diluting each probe in the binding buffer used for DNA immobilization. Since it was necessary to know the amount of DNA immobilized on the particle surface, two additional calibration curves were created specific to each DNA probe. The measurements were conducted using the Qubit ssDNA assay by diluting an 8 μL sample in half with binding buffer and using a 15 μL volume for measurement. By diluting the stock concentrations within the potential range of DNA immobilization, the RFUs generated for each measurement were matched to the calculated, theoretical concentration of copies, as shown in Fig. 3.3.

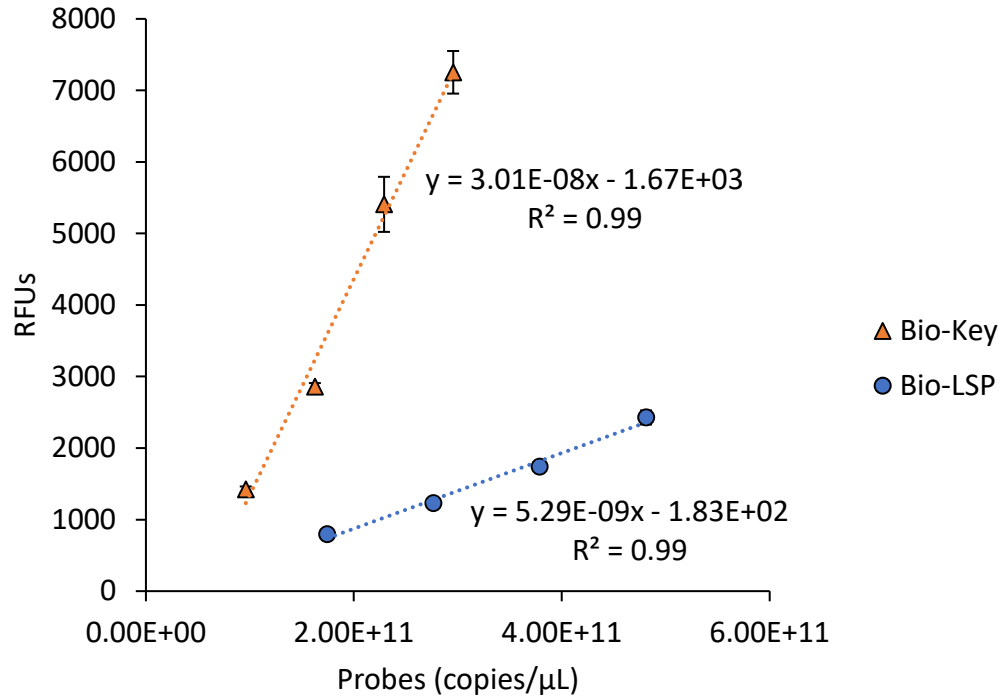


Figure 3.3. Linear calibration of each DNA probe for their quantification after particle immobilization. Samples for each data point were prepared in triplicate, and error bars represent standard deviations.

Quantification of magnetic particles

The microparticles used in this study were Streptavidin Magnetic Particles (Roche, Pleasanton, CA). The particles were provided at a concentration of 10 mg/mL in a solution of 50 mM HEPES, 0.1% bovine serum albumin (BSA), 0.1% chloracetamide, and 0.01% methylisothiazolone at a pH of 7.4. The particles had a 1 μm reported mean diameter and a polystyrene core. To determine if the DNA was immobilizing on the particles in similar copy numbers on the particles, it was necessary to quantify particle recovery after the immobilization process. The optical density values at 500 nm of the particles at 4 different concentrations was measured in a 384 microwell plate using the Epoch 2 microplate spectrophotometer (BioTek Instruments, Inc.,

Winooski, VT), generating a linear calibration curve in the range of 0.1 to 0.4 mg/mL of particles, as shown in Fig. 3.4.

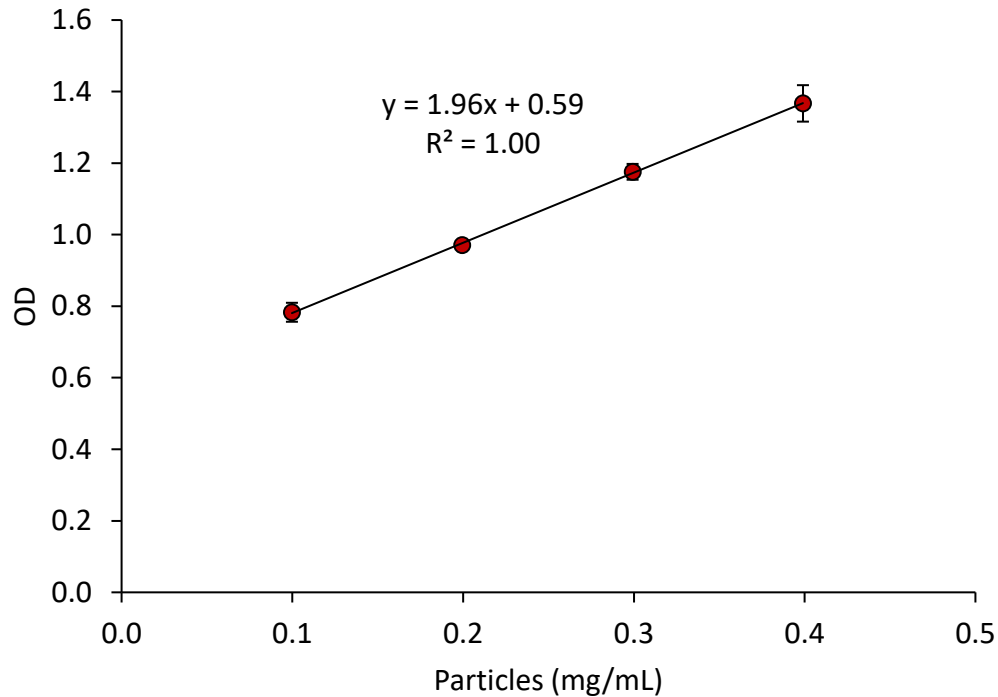


Figure 3.4. Linear calibration for quantification of magnetic particles based on measurement of optical density (OD). Samples for each data point were prepared in triplicate, and the error bars represent standard deviation.

The wavelength for quantification was selected at 500 nm, since DNA did not observe any absorbance that would impact measurements of optical density. For measurements of unknown samples, the samples were diluted prior to measurement accordingly to work within the calibration curve range. Briefly, after immobilization (described in the next section), 10.8 μL of the sample was diluted to a volume of 48 μL with the binding buffer. From that solution, 15 μL were pipetted into 3 different wells for triplicate measurements of the particle concentrations.

Immobilization procedure

A stock solution of particles was created at 2.66 mg/mL by diluting with the binding buffer, which was composed of 10 mM Tris-HCL, 1 mM EDTA, and 100 mM NaCl at a pH of 7.5. Initially, 225 μ L of the particle stock solution was added to 225 μ L of binding buffer. The volume of 450 μ L was maintained throughout the immobilization process. The particles were washed 3 times with 450 μ L of the binding buffer by placing the 1.5 mL centrifuge tubes on a MagneSphere™ Technology Magnetic Separation Stand (Promega, Madison, WI) and pipetting out the supernatant. Each time a sample was placed on the magnetic stand, 5 minutes were allotted for separation to ensure high rates of recovery. The particles were then incubated for 30 minutes with the respective DNA probe in the binding buffer. When added in equivalent concentrations of copies/ μ L, Bio-LSP immobilized more than the Bio-Key. Based on this result and to achieve similar ratios of DNA immobilized per particle mass, less of the Bio-LSP was added during the incubation period. From the stock solution of Bio-Key at a concentration of 4.20×10^{13} copies/ μ L, 103.4 μ L of probe was diluted to the 450 μ L volume, while only 8.34 μ L of the Bio-LSP at a stock concentration of 3.94×10^{13} copies/ μ L was added. During the 30-minute incubation period, the samples were mixed by pipetting every 6 minutes to homogenize and prevent settling of the magnetic particles. After incubation, the supernatant containing unbound DNA was removed by pipetting after placement on the magnetic separator rack, and the particles were washed twice with the wash buffer, which had the same composition and pH as the binding buffer, except with a concentration of 1 M NaCl. The particles were then washed 5 more times with the binding buffer to remove any loosely bound DNA and resuspended in 450 μ L of the same buffer. After the immobilization was complete, the samples were measured for the amount of DNA that immobilized using the Qubit ssDNA assay kit and the calibration curve

shown in Fig. 3.3, as well as the recovered amount of particles using spectrophotometry and the calibration curve shown in Fig. 3.4.

Hybridization procedure of DNA functionalized particles

A reaction volume of 15 μL was used for the hybridization reactions with DNA functionalized particles. The samples were created through the addition of binding buffer, target DNA strand (TS), and the respective particles with immobilized DNA, in that order. The same particle concentrations were used in each hybridization reaction. Conditions that induced the probes to be in similar concentrations were necessary for a direct comparison between probe structures. Therefore, each respective stock of DNA conjugates was diluted to achieve 176 ng/ μL of magnetic particles, yielding an average of 9.00×10^{10} copies/ μL of Bio-Key and 9.48×10^{10} copies/ μL of Bio-LSP in the hybridization reaction. With the concentrations of Bio-LSP probe higher by 4.8×10^9 copies/ μL , additional TS was added to ensure the consistency of tested ratios of TS to probe. These hybridization events with particle-immobilized probes were performed at room temperature to minimize disruption of the biotin-streptavidin complex. During the 1-hour incubation period, the samples were homogenized by pipetting the samples every 10 minutes to prevent any particle settling. At the end of the incubation period, the samples were placed on the magnetic separator for 5 minutes, and then the 15 μL supernatant was removed and placed in a new tube for further analysis. The particles containing hybridized DNA were washed with binding buffer once to remove any loosely bound DNA. After another 5 minutes of magnetic separation, the 15 μL supernatant was once again removed and placed in a new tube. With hybridization complete and all washes obtained, the ssDNA in each supernatant was quantified using the Qubit ssDNA assay using samples of 4 μL . The percent hybridization was calculated by measuring the concentration of TS in the supernatant and subtracting that concentration from

the original TS concentration added. Blanks were created with the probe-functionalized particles but without TS, and exposed to the same hybridization conditions, including the pipetting and washing. For the data presented herein, there was no detectable DNA in the supernatant of the blanks, proving no influence to the samples from extraneous DNA becoming unbound from the particle surface or particles left behind after magnetic separation.

$$\% \text{ Hybridization} = \left(\frac{\text{Original TS Copies} - \text{Measured TS Copies}}{\text{Theoretical Max Hybridized Copies}} \right) \times 100 \quad (2)$$

Statistical Analysis

Initially, all data sets collected were analyzed for normality. The triplicate hybridization data collected from the solution study and the triplicate measurements for the number of probes immobilized displayed normally distributed data. Thus, the data sets were compared via the two-sample t-test to establish significance ($\alpha = 0.05$). For the particle hybridization study, hybridization was conducted in duplicate for each probe structure. Although hybridization data for the immobilized Key displayed normality, the immobilized LSP did not. Therefore, the data sets from the immobilized hybridizations were compared through the nonparametric method of the Wilcoxon rank-sum test to determine significance. Both analyses were conducted using Statistical Analysis Software (SAS) version 9.4.

Results and Discussion

Solution Study

Although the measurements for the all sequences observed increasing RFUs throughout the experiment (Fig. 3.5), the positive slopes exhibited by the scrambled sequences were likely due to background noise that continued to increase as more copies of TS were added. To ensure the observed trends and determined percent hybridizations were not an artifact of the different DNA structures or the excess ssDNA in the samples, probes with the same structures containing

scrambled sequences of bases were placed under the same hybridization conditions and ratios of TS. To compare, linear regressions were conducted for each probe; the linear equation of each probe and R^2 values are shown in Table 3.2.

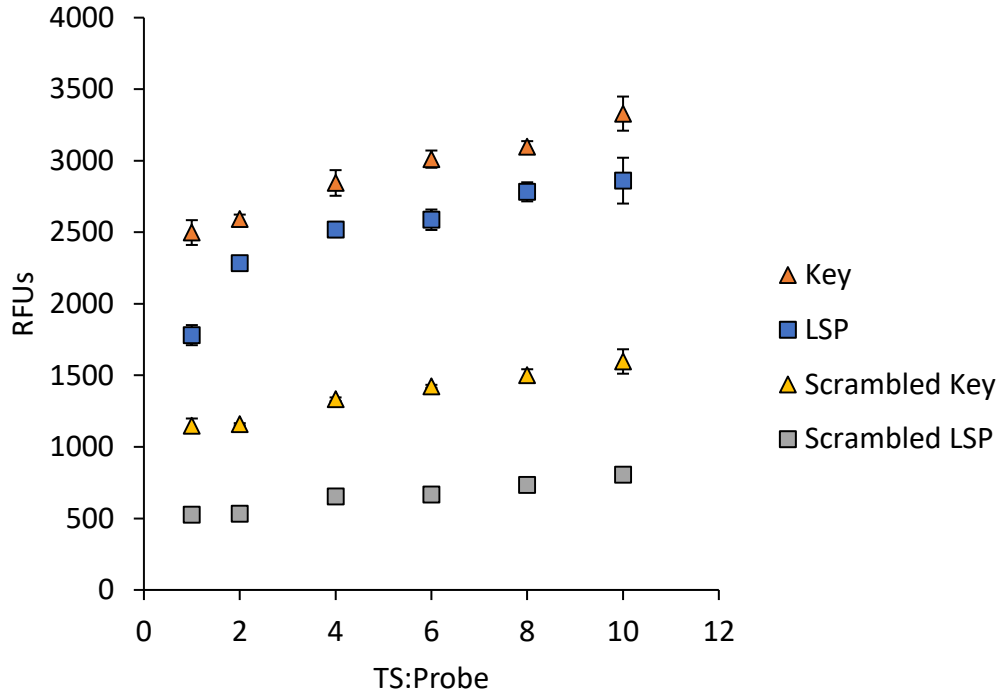


Figure 3.5. Raw RFU measurements from LSP, Key, and the respective scrambled sequences when exposed to incrementally increased copies of TS. Samples were prepared in triplicate for Key and LSP, duplicate for the scrambled sequences, and error bars represent observed standard deviations.

Table 3.2. Linear regressions for the raw RFU measurements associated with each probe at increasing concentration of TS.

Probe	Equation	R^2
Key	$y = 89.39x + 2433.51$	0.98
LSP	$y = 103.17x + 1936.02$	0.83
Scrambled Key	$y = 51.84x + 1091.94$	0.98
Scrambled LSP	$y = 31.12x + 491.76$	0.97

More importantly, the slope of the LSP is 3.32 times greater than that of the scrambled, and the slope of the Key is 1.65 times greater than that of the scrambled. Both probes had steeper slopes than the scrambled counterparts; thus these results demonstrate that the incremental increase in percent hybridization is not purely an artifact of the increased background noise generated at higher ratios of TS to probe, but an increase in hybridized duplexes, and consequently demonstrating the selectivity of these probes to TS.

Furthermore, as seen in the raw values collected, the RFUs emitted by the Key were higher than the LSP, yet the LSP is reported as having higher percent hybridization. Since the Key contained a segment of dsDNA composed of 16 base pairs, a hybridized duplex with the Key contained 46 base pairs, while a hybridized duplex with the LSP only contained 30 base pairs. Therefore, when the RFU values were converted into copies, the number of base pairs in the hybridized sequence was taken into consideration for the calculated percent hybridizations. The ideal duplex formed after hybridization for each probe is shown in Fig. 3.6.



Figure 3.6. Sequences of hybridized duplexes for LSP (top) and Key (bottom) with the probe sequences in black and the TS in red.

The two probes exhibited significantly different percent hybridizations ($p=0.0017$), and overall, the LSP yielded higher percent hybridizations than the Key (Fig. 3.7). The percent hybridization achieved by both DNA probes was determined and plotted against the ratio of available TS to probe copies. Furthermore, hybridization over different ratios of TS to LSP and TS to Key had slopes of 1.88 and 1.06 for the change in percent hybridization over the ratio of

TS to probe, respectively, and R^2 values of 0.83 and 0.98, respectively. This meant not only that the LSP showed higher percent hybridization compared to the Key but also that the LSP was more sensitive to changes in TS concentration. Regardless of the improved hybridization demonstrated by LSP, neither probe displayed percent hybridization that surpassed 44.3%. DNA hybridization is influenced by a variety of conditions, including medium composition (27). These experiments were conducted in ultrapure water, lacking ions that contribute to duplex formation and stability (28). Therefore, if these hybridizations were conducted in a solution of higher ionic strength, the reported percent hybridizations would likely have been higher.

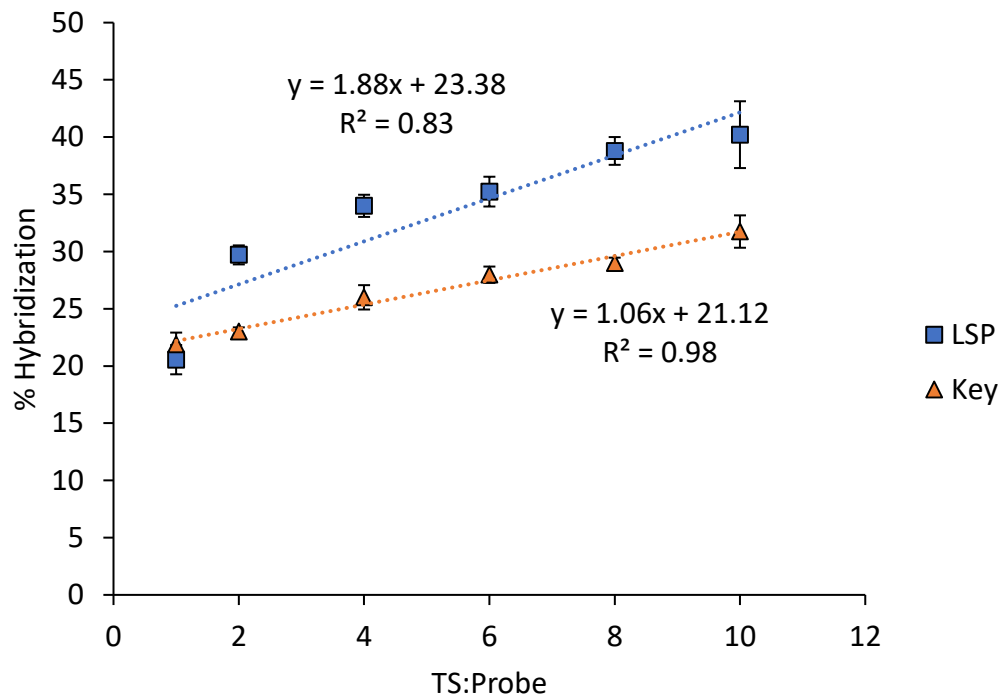


Figure 3.7. Percent hybridization achieved by LSP and Key when exposed to incremental copies of TS. Samples prepared in triplicate, and error bars represent standard deviations.

The reported trends and percent hybridizations were potentially influenced by the lack of monovalent and divalent ions in solution, preventing the desired formation of the Key structure.

Hybridization with dangling-ended DNA structures has been noted as favorable due to lowered

activation energies for the hybridization and increased duplex stability resulting from additional co-axial stacking of DNA (29). However, the Key structure did not present improved percent hybridization compared with the LSP (Fig. 3.7). Depending on the chemistry of the solution and available energy, DNA can take a variety of conformations (30). The efficiency of analyses that require DNA binding, such as PCR analysis, can be affected by the concentration of monovalent and divalent ions. Higher concentrations of magnesium chloride have been noted to coincide with an increase in stability of primer and target DNA (31). It is possible that without a preferable ionic strength of the solution, the Key structure was less likely to form. Although the lack of ions reduced hybridization efficiency, the samples were prepared in ultrapure water to provide a neutral matrix due to the eventual application of enzymes and accompanied buffers. Without the formation of the hairpin structure, the Key could not exhibit beneficial characteristics for hybridization.

To determine the likelihood of desired probe formation, the number of copies of self-hybridized probe was calculated for the scrambled-Key at the 1:1 ratio (Fig. 3.5). Assuming the entire signal was produced via the dsDNA associated with the self-annealing probe, only approximately 20% of the available probe existed in the self-annealed form. Since the Key existed primarily as linear DNA, this would have exposed a sequence of inert DNA and negatively impacted the ability to hybridize. Even short lengths of non-binding sequences can increase the free energy necessary for hybridization to occur (32). Therefore, without formation of the hairpin structure, self-annealing probes, such as the Key, can exhibit binding affinity lower than that of traditional linear DNA probes. The only ratio in which the Key performed comparable to the LSP was the lowest ratio tested; at this ratio, the LSP and Key exhibited percent hybridization of 20.6% and 21.9%, respectively. It is possible that any Key probes in the

preferential form were saturated at this ratio. At higher ratios, the increase in signal for the Key could be attributed to hybridization with the probe in the linear form. The Key present predominantly in the linear form could have been a major contributing factor that reduced the sensitivity of the probe for hybridization.

Characterization of DNA Conjugated Magnetic Particles and Immobilized Hybridization Conditions

When applied at the same concentrations of copies/ μL the Bio-LSP immobilized more copies than the Bio-Key. To achieve similar probe densities on the particle surface, the immobilization procedure required optimization. For a direct comparison between DNA structures, each probe needed to be immobilized in densities as similar to each other as possible. Shifts in probe density have been reported to have a significant impact on sensitivity of sensing mechanisms (33, 34). Thus, the immobilization of the Bio-LSP was conducted at a concentration of 7.31×10^{11} copies/ μL whereas the Key required 9.65×10^{12} copies/ μL . The source of such different immobilization may be due to additional steric hindrance induced by the larger size of the Key (35). With these concentrations optimized, the Bio-LSP and Bio-Key immobilized at ratios of probe to particle mass that were not significantly different ($p = 0.5621$) (Table 3.3). Yet, the immobilization conducted with Bio-Key yielded an average of 17.4% higher recovery of particles, compared to those immobilized with Bio-LSP. Therefore, particle recovery was dependent on the DNA probe. In the context of a biosensor, high particle recovery is important to maintain a reusable system. Higher particle recovery also means higher mass concentration of target DNA, which can improve detection by increasing signal production and most importantly to avoid occurrence of false negatives. In Table 3.3, the lowest concentration of DNA measured was paired with the highest concentration of magnetic particles (MPs) quantified to yield a potential range of copies per mass of particle.

Table 3.3. Characteristics of functionalized magnetic particles (MP) after DNA immobilization. The DNA and magnetic particle concentrations listed are the concentrations recovered after immobilization.

Probe	DNA (copies/ μ L)	MP (mg/mL)	DNA/MP (copies/mg)	Average DNA/MP (copies/mg)
Bio-LSP	4.29×10^{11}	0.87	4.93×10^{14}	5.44×10^{14}
	4.30×10^{11}	0.86	4.99×10^{14}	
	4.48×10^{11}	0.70	6.41×10^{14}	
Bio-Key	5.15×10^{11}	1.08	4.76×10^{14}	5.11×10^{14}
	5.40×10^{11}	1.06	5.11×10^{14}	
	5.42×10^{11}	0.99	5.47×10^{14}	

Particle Study

On average, percent hybridization for the immobilized Bio-LSP was 39.2% and for the Bio-Key was 89.3% (Fig. 3.9). When immobilized both probes displayed higher average percent hybridizations, compared to the unbound probes for the same tested ratios (see solution study section and Fig. 3.7). The hybridization experiments for the DNA immobilized on the particle surfaces were conducted in a saline buffer in which secondary structure was favorable, unlike the solution-phase DNA hybridizations that were performed in ultrapure water. Therefore, the water chemistry conditions in the samples were more suited for hybridization in the particle study, which is a potential reason for the higher percentages of hybridization reported for the immobilized DNA.

Another difference was the methodology applied to quantify hybridization. The data displayed in Fig. 3.9 was calculated via Equation 2. Since the concentration for possible hybridization was only 2.54 ng/ μ L, small changes could have been difficult to clearly discern at the high concentrations tested and multiple measurements for the higher tested ratios were close

to the upper limit of quantification, which is a potential reason for the large fluctuations in the measured values.

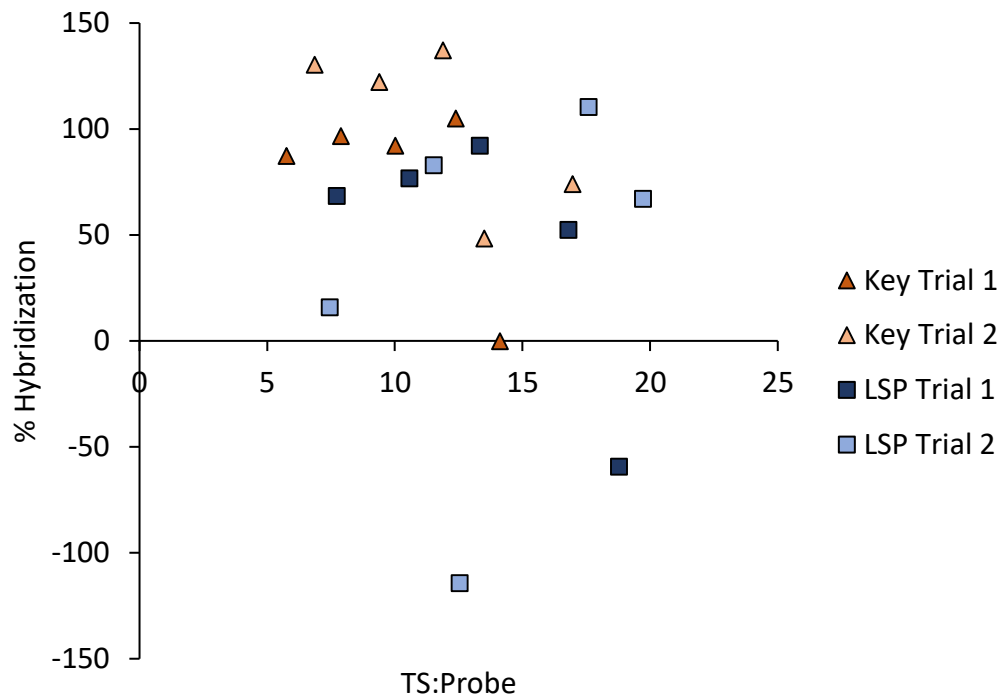


Figure 3.8. Hybridization efficiency for DNA immobilized (Bio-Key and Bio-LSP) on particles at increasing availability of DNA target sequence (TS).

Unlike the solution experiment, the hybridization observed between the two immobilized probes was not statistically different ($p=0.0630$), suggesting that the presence of secondary structure had no direct effect on hybridization when probes were immobilized. Furthermore, the sample conditions during the particle study were conducive to the formation of the hairpin structure, unlike the solution study. An online server called Mfold was utilized to analyze the potential conformations of both the LSP and Key (36), which showed that the activation energies for all proposed DNA conformations of the LSP were positive and would not have occurred spontaneously without the input of energy. For the Key, based on conditions that the samples experienced during hybridization, the hairpin structure was favored for spontaneous formation,

with negative activation energy. This opposes the findings of a previous study by Riccelli et al. (21) that observed improved rates of hybridization and binding affinity with dangling-ended hairpin probes compared to linear probes when immobilized on a planar surface. However, the curvature of the surface on which probes are immobilized has been noted to influence hybridization. In fact, particle surfaces have been described as alternative supports to planar substrates because they can provide homogenous surfaces for immobilization and hybridization, increased surface area, and faster binding kinetics (37–39). Even though other factors, such as probe density, could alter the binding affinities observed, for the probe density tested, there was no statistically significant difference in hybridization between the immobilized DNA structures.

Conclusions

DNA hybridization was studied for two different DNA structures both in solution and immobilized on a particle surface. The reported data provided practical information in terms of probe application within a biosensor. Biosensors that incorporate hybridization of unbound DNA in low ionic conditions could benefit from application of linear DNA probes, opposed to structured ones. The probes tested in the solution study suggested the importance of ionic strength in solution for the prevalence of secondary structure. For unbound DNA probes, the linear structure observed higher hybridization than the Key, as a result of shifts in DNA conformational structure due to unfavorable ionic conditions. However, the factors controlling hybridization were likely completely different when the DNA probes were immobilized. Unlike the solution study, changes in the DNA structure did not have a significant influence over hybridization for the experiments conducted on immobilized DNA probes. However, during magnetic separation, larger DNA structures immobilized on the surface increased particle recovery. Thus, even though neither immobilized probe displayed significantly higher percentages of hybridization, the Key would create a more sustainable and reusable sensing

mechanism. More importantly, higher particle recovery demonstrated by the particles functionalized with the Key could more readily concentrate targeted DNA sequences, increase signal production, and reduce occurrence of false negatives, compared to immobilized sequences of smaller structure. Ultimately, immobilizing DNA and hybridizing in buffered conditions could lead to more sensitive and functional biosensors compared to conducting hybridization in solution at low ionic strength.

References

1. Capodaglio, A.G., Callegari, A. and Molognoni, D. (2016) Online monitoring of priority and dangerous pollutants in natural and urban waters: A state-of-the-art review. *Manag. Environ. Qual. An Int. J.*, **27**, 507–536.
2. Wang, H., Bédard, E., Prévost, M., Camper, A.K., Hill, V.R. and Pruden, A. (2017) Methodological approaches for monitoring opportunistic pathogens in premise plumbing: A review. *Water Res.*, **117**, 68–86.
3. Rogers, K.R. and Gerlach, C.L. (1996) Environmental biosensors: A status report. *Environ. Sci. Technol.*, **30**.
4. Mehrotra, P. (2016) Biosensors and their applications - A review. *J. Oral Biol. Craniofacial Res.*, **6**, 153–159.
5. Velusamy, V., Arshak, K., Korostynska, O., Oliwa, K. and Adley, C. (2010) An overview of foodborne pathogen detection: In the perspective of biosensors. *Biotechnol. Adv.*, **28**, 232–254.
6. Zeng, L., Wang, L. and Hu, J. (2018) Current and Emerging Technologies for Rapid Detection of Pathogens. In *Biosensing Technologies for the Detection of Pathogens - A Prospective Way for Rapid Analysis*. pp. 5–19.
7. Lucarelli, F., Tombelli, S., Minunni, M., Marrazza, G. and Mascini, M. (2008) Electrochemical and piezoelectric DNA biosensors for hybridisation detection. *Anal. Chim. Acta*, **609**, 139–159.
8. Goode, J.A., Rushworth, J.V.H. and Millner, P.A. (2015) Biosensor Regeneration: A Review of Common Techniques and Outcomes. *Langmuir*, **31**, 6267–6276.
9. Cotruvo, J.A., Purkiss, D., Hazan, S., Sidari, F.P., DeMarco, P. and LeChevallier, M. (2019) Managing Legionella and Other Pathogenic Microorganisms in Building Water Systems. *J. Am. Water Works Assoc.*, **111**, 54–59.
10. Centers for Disease Control and Prevention (2018) *Legionella: History, Burden, and Trends*.

11. Donohue, M.J., O'Connell, K., Vesper, S.J., Mistry, J.H., King, D., Kostich, M. and Pfaller, S. (2014) Widespread Molecular Detection of *Legionella pneumophila* Serogroup 1 in Cold Water Taps across the United States. *Environ. Sci. Technol.*, **48**, 3145–3152.
12. Laschi, S., Miranda-Castro, R., González-Fernández, E., Palchetti, I., Reymond, F., Rossier, J.S. and Marrazza, G. (2010) A new gravity-driven microfluidic-based electrochemical assay coupled to magnetic beads for nucleic acid detection. *Electrophoresis*, **31**, 3727–3736.
13. Rai, V., Deng, J. and Toh, C.S. (2012) Electrochemical nanoporous alumina membrane-based label-free DNA biosensor for the detection of *Legionella sp.* *Talanta*, **98**, 112–117.
14. Miranda-Castro, R., de-los-Santos-Álvarez, N., Lobo-Castañón, M.J., Miranda-Ordieres, A.J. and Tuñón-Blanco, P. (2009) PCR-coupled electrochemical sensing of *Legionella pneumophila*. *Biosens. Bioelectron.*, **24**, 2390–2396.
15. Wetmur, J.G. and Fresco, J. (1991) DNA probes: Applications of the principles of nucleic acid hybridization. *Crit. Rev. Biochem. Mol. Biol.*, **26**, 227–259.
16. Liu, A., Wang, K., Weng, S., Lei, Y., Lin, L., Chen, W., Lin, X. and Chen, Y. (2012) Development of electrochemical DNA biosensors. *TrAC - Trends Anal. Chem.*, **37**, 101–111.
17. Miranda-Castro, R., De-Los-Santos-Álvarez, P., Lobo-Castañón, M.J., Miranda-Ordieres, A.J. and Tuñón-Blanco, P. (2007) Hairpin-DNA probe for enzyme-amplified electrochemical detection of *Legionella pneumophila*. *Anal. Chem.*, **79**, 4050–4055.
18. Chen, C., Wang, W., Wang, Z., Wei, F. and Zhao, X.S. (2007) Influence of secondary structure on kinetics and reaction mechanism of DNA hybridization. *Nucleic Acids Res.*, **35**, 2875–2884.
19. Gao, Y., Wolf, L.K. and Georgiadis, R.M. (2006) Secondary structure effects on DNA hybridization kinetics: A solution versus surface comparison. *Nucleic Acids Res.*, **34**, 3370–3377.
20. Miranda-Castro, R., De-los-Santos-Álvarez, N., Lobo-Castañón, M.J., Miranda-Ordieres, A.J. and Tuñón-Blanco, P. (2009) Structured nucleic acid probes for electrochemical devices. *Electroanalysis*, **21**, 2077–2090.
21. Riccelli, P. V, Merante, F., Leung, K.T., Bortolin, S., Zastawny, R.L., Janeczko, R. and Benight, A.S. (2001) Hybridization of single-stranded DNA targets to immobilized complementary DNA probes: comparison of hairpin versus linear capture probes. *Nucleic Acids Res.*, **29**, 996–1004.
22. Ravan, H., Kashanian, S., Sanadgol, N., Badoei-Dalfard, A. and Karami, Z. (2014) Strategies for optimizing DNA hybridization on surfaces. *Anal. Biochem.*, **444**, 41–46.

23. Riccelli, P. V., Mandell, K.E. and Benight, A.S. (2002) Melting studies of dangling-ended DNA hairpins: effects of end length, loop sequence and biotinylation of loop bases. *Nucleic Acids Res.*, **30**, 4088–4093.
24. Nwokeoji, A.O., Kilby, P.M., Portwood, D.E. and Dickman, M.J. (2017) Accurate Quantification of Nucleic Acids Using Hypochromicity Measurements in Conjunction with UV Spectrophotometry. *Anal. Chem.*, **89**, 13567–13574.
25. Zang, Y., Lei, J., Ling, P. and Ju, H. (2015) Catalytic hairpin assembly-programmed porphyrin-DNA complex as photoelectrochemical initiator for DNA biosensing. *Anal. Chem.*, **87**, 5430–5436.
26. AAT Bioquest. (2019) Amplite™ Colorimetric Biotin Quantitation.
27. Liebermann, T., Knoll, W., Sluka, P. and Herrmann, R. (2000) Complement hybridization from solution to surface-attached probe- oligonucleotides observed by surface-plasmon-field-enhanced fluorescence spectroscopy. *Colloids Surfaces A Physicochem. Eng. Asp.*, **169**, 337–350.
28. Owczarzy, R., Moreira, B.G., You, Y., Behlke, M.A. and Walder, J.A. (2008) Predicting stability of DNA duplexes in solutions containing magnesium and monovalent cations. *Biochemistry*, **47**, 5336–5353.
29. Lane, M.J., Paner, T., Kashin, I., Faldasz, B.D., Li, B., Gallo, F.J. and Benight, A.S. (1997) The thermodynamic advantage of DNA oligonucleotide ‘stacking hybridization’ reactions: Energetics of a DNA nick. *Nucleic Acids Res.*, **25**, 611–616.
30. SantaLucia, J. and Hicks, D. (2004) The Thermodynamics of DNA Structural Motifs. *Annu. Rev. Biophys. Biomol. Struct.*, **33**, 415–440.
31. Henegariu, O., Heerema, N.A., Dlouhy, S.R., Vance, G.H. and Vogt, P.H. (1997) Multiplex PCR: Critical Parameters and Step-by-Step Protocol. *Biotechniques*, **23**.
32. Di Michele, L., Mognetti, B.M., Yanagishima, T., Varilly, P., Ruff, Z., Frenkel, D. and Eiser, E. (2014) Effect of inert tails on the thermodynamics of DNA hybridization. *J. Am. Chem. Soc.*, **136**, 6538–6541.
33. Peng, H., Soeller, C., Travas-Sejdic, J. and Kjallman, T.H.M. (2008) Effect of Probe Density and Hybridization Temperature on the Response of an Electrochemical Hairpin-DNA Sensor. *Anal. Chem.*, **80**, 9460–9466.
34. Macedo, L.J.A., Miller, E.N. and Opdahl, A. (2017) Effect of Probe-Probe Distance on the Stability of DNA Hybrids on Surfaces. *Anal. Chem.*, **89**, 1757–1763.
35. Steichen, M. and Buess-Herman, C. (2005) Electrochemical detection of the immobilization and hybridization of unlabeled linear and hairpin DNA on gold. *Electrochem. commun.*, **7**, 416–420.

36. Zuker,M. (2003) Mfold web server for nucleic acid folding and hybridization prediction. *Nucleic Acids Res.*, **31**, 3406–3415.
37. Spiro,A., Lowe,M. and Brown,D. (2000) A bead-based method for multiplexed identification and quantitation of DNA sequences using flow cytometry. *Appl. Environ. Microbiol.*, **66**, 4258–4265.
38. Son,A., Dosev,D., Nichkova,M., Ma,Z., Kennedy,I.M., Scow,K.M. and Hristova,K.R. (2007) Quantitative DNA hybridization in solution using magnetic/luminescent core-shell nanoparticles. *Anal. Biochem.*, **370**, 186–194.
39. Jennings,T.L., Rahman,K.S., Fournier-Bidoz,S. and Chan,W.C.W. (2008) Effects of microbead surface chemistry on DNA loading and hybridization efficiency. *Anal. Chem.*, **80**, 2849–2856.

CHAPTER 4. GENERAL CONCLUSIONS

The spread of disease via waterborne pathogens continues to threaten potable water across the world. Building and optimizing monitoring devices to detect such pathogens are vital for the future of water security and public health. Current pathogenic monitoring practices of culturing are antiquated, and at times, inaccurate. Point-of-care (POC) sensing mechanisms that provide *in situ* monitoring would allow for faster response to outbreaks and make water quality public knowledge. DNA-based biosensors have displayed the ability to conduct selective, specific, and long-term monitoring of dangerous pathogens. Optimizing current DNA-based biosensing technologies is an important step to increase sensitivity and push the devices closer to commercialization.

The overarching goal of this research was to better understand the application of DNA hybridization as a bioreceptor by providing a comparative analysis of DNA hybridization observed for linear and dangling-ended hairpin probes, both in solution and immobilized on a microparticle surface. Through this M.S. research, improved DNA quantification methods were developed based on chemical and enzymatic treatment in conjunction with Qubit fluorometric assays. Available forms of DNA quantification are not sensitive or selective enough to ensure accurate measurement when the samples contain a mixture of both ssDNA and dsDNA. A working solution composed of DMSO mixed with the buffer and dye provided in the Qubit ssDNA Assay Kit was shown to allow for dye binding, while creating a chemical matrix that induced and sustained denaturation. This methodology was essential to accurately quantify copies of DNA probes with sections of both ssDNA and dsDNA. In addition, application of exonuclease I and alkaline phosphatase were effective for isolating dsDNA and determining

hybridization, even in solutions containing concentrations of ssDNA over 80x that of the dsDNA.

Engineering Significance

More importantly, the developed DNA quantification methodologies were ultimately applied to study the hybridization of linear and dangling-ended hairpin DNA probes in solution. The linear probe yielded more hybridized duplexes than the structured probe, when the complementary strand was present at least double that of the probe. However, the observed lower percentages of hybridization demonstrated by the dangling-ended hairpin probe could have been a result of the experiment being conducted in ultrapure water, without ions that encourage the hairpin structure to form. This comparative study suggested the importance of ionic strength when using DNA as a bioreceptor. More importantly, the study exhibited linear ssDNA better suited for hybridization in samples absent of ions strength whereas structured probes are more dependent on ionic conditions for hybridization. However, once the probes were immobilized on a microparticle surface, the difference in hybridization observed for both probes was not statistically significant. Therefore, based on the collected data, the presence or absence of secondary structure did not have an influence on hybridization, after the probes were immobilized. If immobilizing DNA probes on a microparticle, simplistic linear DNA probes may be just as effective as complex structured probes for hybridization. However, during immobilization, the larger, structured probe recovered over 17.4% more particles after magnetic concentration. Therefore, larger DNA structures might yield higher recovery rates of particles and be a more sustainable bioreceptor. Furthermore, in the conditions tested, the immobilized probes overall observed higher hybridization percentages. As seen in Fig. 4.1, this research has focused on the preliminary incubation or reaction necessary to produce a signal in a biosensor.

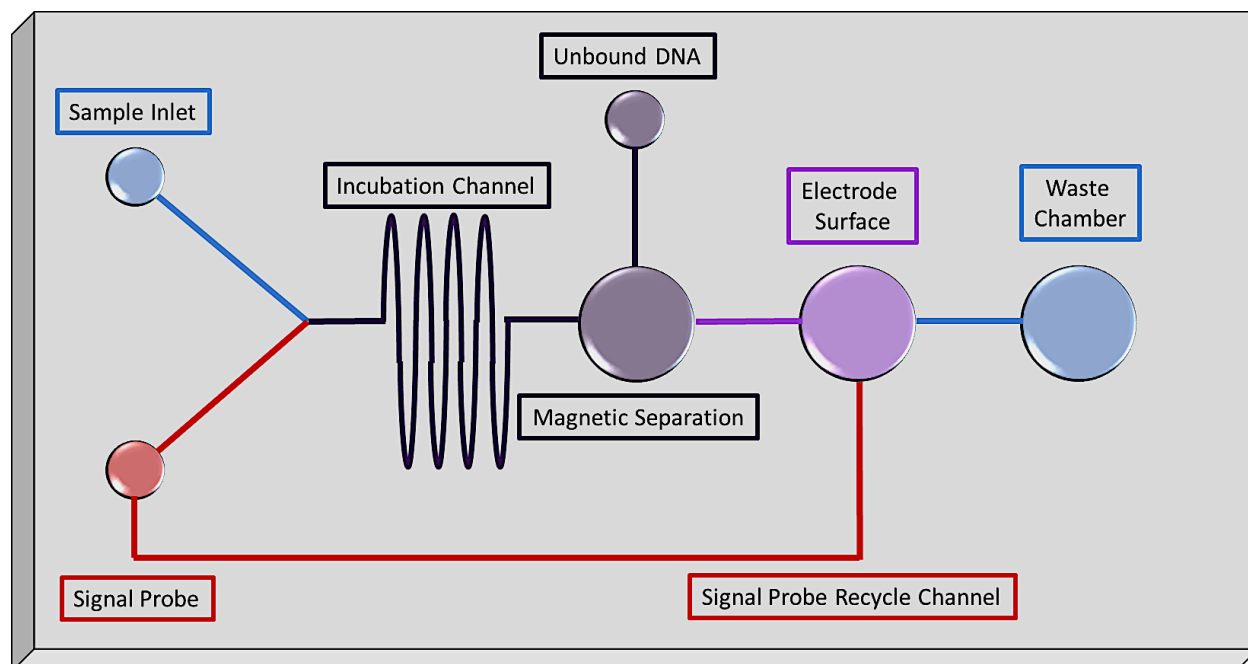


Figure 4.1. Schematic of microfluidic device enabled for magnetic separation followed by electrochemical biosensing enabled for magnetic separation

Future Recommendations

As displayed by the complications for structured DNA when changing sample matrix, the enzymes applied for digestion of ssDNA need to be reviewed for enzymatic activity in matrices of other chemical composition. For the methodology presented to be more robust, the chemical composition of the sample needs to remain as consistent as possible, even during measurement. Therefore, the current enzymes applied should be reviewed and potentially replaced by more robust enzymes.

The dangling-ended hairpin probe synthesized for this research, requires further attention and study. If conformational shifts by the probe are possible, hybridization with target DNA can be controlled by changing the ionic strength of the sample. Controlling the capture and release of target DNA without the use of harsh chemicals or heat could prove to be a powerful bioreceptor.

More replicates of the hybridization experiment with the immobilized probes are necessary to assist in removal of any outliers collected during the process and potentially confirm the observed result of structure not influencing hybridization on a microparticle surface. In addition, more experimentation is also necessary to determine and identify the variables affecting particle recovery. In the confines of this study, probe size appeared to be a major influence during the immobilization of DNA. A more rigorous analysis of the influence of immobilized probe size and structure on particle recovery should be conducted. A study such as this could potentially lead to improved detection by optimizing the concentration of target DNA through magnetic separation and more sustainable biosensors with a longer lifecycle.

APPENDIX. PCR PROTOCOLS

Table A.1. PCR primers and protocols for detection of OPPPs.

Genus/Species	Target Gene(s)	Primer Names	Primer Sequence (5'-3')	Initial Denaturation and Enzyme Activation (temperature & time)	Denaturing, Annealing, and Extension (Cycles, temperature, & time)	Reference
<i>Legionella</i> spp.	23S rRNA	Leg23SF Leg23SR	CCCATGAAGCCCGTTGAA ACAATCAGCCAATTAGTACGAGTTAGC	95 °C for 2 min	40 cycles of 95°C for 5 s and 58.5°C for 10 s	(1)
<i>L. pneumophila</i>	<i>mip</i>	LmipF LmipR	AAAGGCATGCAAGACGCTATG GAAACTTGTTAAGAACGTCTTTCATTTG	95 °C for 2 min	40 cycles of 95°C for 5 s and 50°C for 10 s	(1)
<i>Mycobacterium</i> spp.	16S rRNA	110F 1571R	CCTGGGAAACTGGGTCTAAT CGCAGCTCACAGTTA	95 °C for 2 min	45 cycles of 95°C for 5 s, 55°C for 15 s, and 72°C for 10 s	(1)
<i>M. avium</i>	16S rRNA	MycavF MycavR	AGAGTTTGATCCTGGCTCAG ACCAGAAGACATGCGTCTTG	98 °C for 2 min	40 cycles of 98°C for 5 s and 68°C for 18 s	(1)
<i>P. aeruginosa</i>	<i>ecfX</i> & <i>gyrB</i>	ecfXF ecfXR gyrBF gyrBR	CGCATGCCTATCAGGCGTT GAACTGCCCAGGTGCTTGC CCTGACCATCCGTCGCCACAAC CGCAGCAGGATGCCGACGCC	95 °C for 2 min	50 cycles of 95°C for 5 s and 60°C for 10 s	(1)

Table A.1. Continued

Genus/Species	Target Gene(s)	Primer Names	Primer Sequence (5'-3')	Initial Denaturation and Enzyme Activation (temperature & time)	Denaturing, Annealing, and Extension (Cycles, temperature, & time)	Reference
<i>Methylobacterium</i> spp.	16S rRNA	MB4 MB	CCGCGTGAGTGATGAAGG AGCGCCGTCGGGTAAGA	94 °C for 5 min	4 cycles of 94°C for 60 s, 62°C for 60 s, and 72°C for 3 min; repeat 4 cycles with new annealing temp of 60°C, and 30 more times with annealing temp of 58°C	(2)
<i>A. baumannii</i>	<i>ompA</i>	OmpAF OmpAR	TCTTGGTGGTCACTTGAAGC ACTCTTGTGGTTGTGGAGCA	50 °C for 2 min and 95 °C for 10 min	38 cycles of 95°C for 30 s and 62°C for 60 s	(3)
<i>A. hydrophila</i>	16S rRNA	AH16SF AH16SR	GAAAGGTTGATGCCTAATACGTA CGTGCTGGCAACAAAGGACAG	95 °C for 2.5 min	35 cycles of 94°C for 30 s, 57°C for 60 s, 72°C for 5 min	(4)

References

1. Wang,H., Edwards,M., Falkinham,J.O. and Pruden,A. (2012) Molecular survey of the occurrence of *Legionella* spp., *Mycobacterium* spp., *Pseudomonas aeruginosa*, and amoeba hosts in two chloraminated drinking water distribution systems. *Appl. Environ. Microbiol.*, **78**, 6285–6294.
2. Podolich,O., Lashevskyy,V., Ovcharenko,L., Kozyrovska,N. and Pirttilä,A.M. (2009) *Methylobacterium* sp. resides in unculturable state in potato tissues in vitro and becomes culturable after induction by *Pseudomonas fluorescens* IMGB163. *J. Appl. Microbiol.*, **106**, 728–737.
3. McConnell,M.J., Pérez-Ordóñez,A., Pérez-Romero,P., Valencia,R., Lepe,J.A., Vázquez-Barba,I. and Pachón,J. (2012) Quantitative real-time PCR for detection of *Acinetobacter baumannii* colonization in the hospital environment. *J. Clin. Microbiol.*, **50**, 1412–1414.
4. Pandove,G., Sahota,P.P., Achal,V. and Vikal,Y. (2011) Detection of *Aeromonas hydrophila* in water using PCR. *J. Am. Water Works Assoc.*, **103**, 59–65.